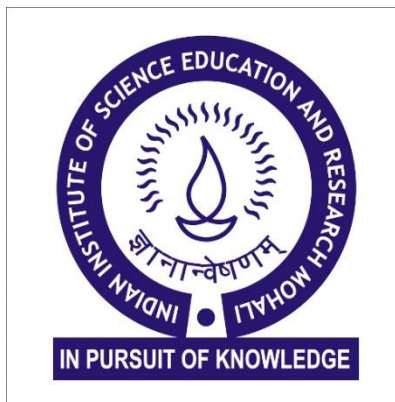


# **Synthesis and Characterization of Red Emitting TICT Rotors for Monitoring of Mitochondrial Microenvironment**

**LOPAMUDRA DAS**

*A dissertation submitted for the partial fulfilment of BS-MS dual degree  
in science.*



**Indian Institute of Science Education and Research, Mohali**

**May 2020**

## Certificate of Examination

This is to certify that the dissertation titled “**Synthesis and characterization of red emitting TICT rotors for monitoring of mitochondrial microenvironment**” submitted by Ms Lopamudra Das (Reg. No. MS15167) for the partial fulfillment of BS-MS dual degree programme of the Institute, has been examined by the thesis committee duly appointed by the Institute. The committee finds the work done by the candidate satisfactory and recommends that the report be accepted.

Dr. Sugumar Venkataramani

Assistant Professor

IISER Mohali

Dr. Raj Kumar Roy

Assistant Professor

IISER Mohali

Dr. Sanchita Sengupta

Assistant Professor

IISER Mohali

(Supervisor)

Dated:

May 4, 2020

## **Declaration**

The work presented in this dissertation has been carried out by me under the guidance of Dr.Sanchita Sengupta at the Indian Institute of Science Education and Research Mohali.

This work has not been submitted in part or in full for a degree, a diploma, or a fellowship to any other university or institute. Whenever contributions of others are involved, every effort is made to indicate this clearly, with due acknowledgement of collaborative research and discussions. This thesis is a bonafide record of original work done by me and all sources listed within have been detailed in the bibliography.

Lopamudra Das

(Candidate)

Dated: May 4, 2020

In my capacity as the supervisor of the candidate's project work, I certify that the above statements by the candidate are true to the best of my knowledge.

Dr. Sanchita Sengupta

(Supervisor)

## **Acknowledgement**

I want to express my deepest thanks to my guide Dr. Sanchita Sengupta for the continuous guidance, support and instructive discussions and valuable advise that she has provided me throughout the course of my project. I am deeply thankful and grateful to her for believing in me and giving me this wonderful opportunity to work in her group.

I wish to thank my committee members Dr. Sugumar Venkataramani and Dr. Raj Kumar Roy for giving valuable suggestions and questions during the thesis discussions..

Thanks a lot to my lab members Narendra, Sushil, Kavita, Anita and Nahas for their help, support and immense knowledge sharing. Thanks for keeping motivated and providing a friendly atmosphere. I would also like to thank RKR group members Arjun, Deepak, Umer, Subhendu, Ankita, Dr. Shiv for their help, support and maintaining a cheerful, comfortable and enjoyable atmosphere.

And thanks to all of my friends who were there for help and motivation. Thanks to Megha, Sunandini, Shweta, Lincoln, Prashant, Raman, Srishti, Anjana for being there for me.

Special thanks to my brother for keeping me motivated and giving life lessons.

A lot of thanks to my parents and my whole family for their love, care, trust, help, motivation, support and for everything they have given. I'm really blessed to have each one of them in my life.

# Contents

|                                       |      |
|---------------------------------------|------|
| List of Figures.....                  | vi   |
| List of Tables.....                   | viii |
| List of Scheme.....                   | ix   |
| List of Abbreviations.....            | xi   |
| Abstract.....                         | 1    |
| Chapter 1: Introduction.....          | 2    |
| Chapter 2: Result and Discussion..... | 20   |
| Chapter 3: Summary and Outlook.....   | 26   |
| Chapter 4: Experimental Section.....  | 29   |
| References.....                       | 49   |
| Appendix.....                         | 51   |

## List of Figures

**Fig.1.1.** The general photophysical mechanism of Donor-Acceptor fluorophores undergoing TICT phenomenon.

**Fig.1.2.** Illustrative structure of a TICT active rotor based on electron donor acceptor systems (A) displaying the electron donating moiety (green), the electron accepting moiety and the electron rich spacer (blue). Basic examples are (B) 1,4-dimethylamino benzonitrile (DMABN), (C) 9-(dicyanovinyl) julolidine (DCVJ) and (D) p-(dimethylamino) stilbazolium (p-DASPMI)..

**Fig 1.3.** Schematic outline behind the operation of viscosity based TICT active molecular rotors.

**Fig 1.4.** Examples of BODIPY based FMRs with chemically functionalized meso-phenyl ring in the presence of different substituents.

**Fig 1.5.** The structural diagram and emission characteristics (in increasing viscosity) of a viscosity responsive rotor linked to a non-responsive reference rotor (CMAM-MCAA) based on ratiometric detection approach.

**Fig 1.6.** Fluorescence molecular rotor with displaying temperature responsive attributes.

**Fig 1.7.** Lifetime evaluation graph of BODIPY C<sub>10</sub> at different viscosity and temperature conditions.

**Fig 1.8.** General illustration of two well known pathways for the layout of a mitochondrial targeting functionalized chromophore.

**Fig 1.9.** Fundamental examples of positively charged mitochondrial specific group functionalized fluorophore.

**Fig 1.10.** (A) BODIPY Vis A rotor showing the working principle of immobilization onto the mitochondria. (B) The bio-imaging of BODIPY Vis A viscosity rotor and Mitotracker DeepRed inside mitochondria in the absence and presence of formahaldehyde.

**Fig 1.11.** General mechanism behind the working of the Lyso-V molecular rotor.

**Fig 1.12.** Structures of DEAB-TO-3 and TO-3 Nucleus Localized Probe.

**Fig 1.13.** Representative molecular design of regioisomeric dyads *p-AD* and *m-AD* and ADA triads *m-ADA*, *p-ADA* prepared and studied in this work

**Fig 1.14.** Correlation of absorption spectra for *m-AD*, *m-ADA*, and *p-AD* in chloroform ( $c=10^{-5}$  M); b) Normalized emission spectra for *m-AD*, *p-AD*, and *m-ADA* in  $\text{CHCl}_3$  ( $c=10^{-5}$  M) upon exciting at 362 nm, 377 nm and 380 nm, respectively.

**Fig 1.15.** Emission spectra of dyads a) *p-AD* and b) *m-AD*, and triads c) *p-ADA* and d) *m-ADA* in solution various viscosities

**Fig 1.16.** .Molecular design adopted in this project.

## List of Tables

**Table 4.1.** Various standardization methods to prepare 2,6-Dibromobenzo[1,2-b;4,5-b']dithiophene-4,8-dione

**Table 4.2.** Various optimization methods for the synthesis of 1,1'-[4,8-bis[(6-bromohexyl)oxy]benzo[1,2-b:4,5-b']dithiophene-2,6-diyl]bis[1,1,1-trimethyl-stannate.

**Table 4.3.** Various optimization methods for the synthesis of 1,1'-[4,8-bis[(6-bromohexyl)oxy]benzo[1,2-b:4,5-b']dithiophene-2,6-diyl]bis[1,1,1-trimethyl-stannate.

**Table 4.4.** Various standardization methods (trial reactions) to prepare 2,6-Dibromobenzo[1,2-b;4,5-b']dithiophene-4,8-dione.



## List of Schemes

**Scheme 2.1.** Synthesis of 4,8-Bis(6-bromohexyl)benzo[1,2-b:4,5-b']dithiophene from BDT-diol.

**Scheme 2.2.** Synthesis of 4,8-Bis(6-bromohexyl)benzo[1,2-b:4,5-b']dithiophene from BDT-dione.

**Scheme 2.3.** Synthesis of 4,8-Bis(6-(1-hexyloxy)piperidine)benzo[1,2-b:4,5b']dithiophene from BDT-dione.

**Scheme 2.4.** Synthetic scheme for the synthesis of ADA-1 compound.

**Scheme 2.5.** Schematic diagram for the Synthesis of ADA-2 compound (reference compound).

**Scheme 2.6.** Synthesis of 1,1'-[4,8-bis[(6-bromohexyl)oxy]benzo[1,2-b:4,5-b']dithiophene-2,6-diyl]bis[1,1,1-trimethyl-stannate.

**Scheme 2.7.** Synthesis of 8-(2-bromothien-5-yl)-3,5-dimethyl-4,4-difluoro-4-bora-3a,4a-diaza-s-indacene (BODIPY).

**Scheme 4.1.** Synthesis of (*N,N*-diethyl)thiophenecarboxylamide.

**Scheme 4.2.** Synthesis of Benzo[1,2-b:4,5-b']dithiophene-4,8-dione (BDT-dione).

**Scheme 4.3.** Synthesis of 4,8-Bis(hydroxy)benzo[1,2-b:4,5-b']dithiophene(BDT diol).

**Scheme 4.4.1.** Synthesis of 4,8-Bis[(6-bromohexyl)oxy]benzo[1,2-b:4,5-b']dithiophene from BDT-diol.

**Scheme 4.4.2.** Synthesis of 4,8-Bis[(6-bromohexyl)oxy]benzo[1,2-b:4,5-b']dithiophene from BDT-dione using water as the solvent.

**Scheme 4.4.3.** Synthesis of 4,8-Bis[(6-bromohexyl)oxy]benzo[1,2-b:4,5-b']dithiophene from BDT-dione using water and THF as the solvent and using sodium dithionite as the reducing agent.

**Scheme 4.4.4.** Synthesis of 4,8-Bis[(6-bromohexyl)oxy]benzo[1,2-b:4,5-b']dithiophene from

BDT-dione using water and DMSO as the solvent and using  $K_2CO_3$  as a mild base.

**Scheme 4.4.5.** Synthesis of 4,8-Bis[(6-bromohexyl)oxy]benzo[1,2-b:4,5-b']dithiophene from BDT-dione using water and ethanol as the solvent and using NaOH as a strong base.

**Scheme 4.5.** Synthesis of 1-(6-bromohexyl)piperidine.

**Scheme 4.6.** Synthesis of 4,8-Bis(6-(1-hexyloxy)piperidine)benzo[1,2-b:4,5b']dithiophene.

**Scheme 4.7.** Synthesis of 4,8-Bis(6-(1-hexyloxy)piperidine)benzo[1,2-b:4,5b']dithiophene.

**Scheme 4.8.** Synthesis of donor molecule with piperidine targeting group.

**Scheme 4.9.** Synthesis of alkylated Benzodithiophene.

**Scheme 4.10.** Synthesis of (4,8-di(oct-1-yn-1-yl)benzo[1,2-b:4,5-b']dithiophene-2,6-diyl)bis(trimethylstannane) donor molecule with no targeting group.

**Scheme 4.11.** Synthesis of 1,1'-[4,8-bis[(6-bromohexyl)oxy]benzo[1,2-b:4,5-b']dithiophene-2,6-diyl]bis[1,1,1-trimethyl-stannate].

**Scheme 4.12.** Synthesis of 2,5-Dibromo-N,N-diethylthiophene 3-Carboxamide.

**Scheme 4.13.** Synthesis of 2,5-Diiodo-N,N-diethylthiophene 3-Carboxamide.

**Scheme 4.14.** Synthesis of 2,6-Dibromobenzo[1,2-b:4,5-b']dithiophene-4,8-dione.

**Scheme 4.15.1.** Synthesis of methyl pyrrole from pyrrole.

**Scheme 4.15.2.** Synthesis of methyl-pyrrole from Pyrrole 2-carboxyaldehyde.

**Scheme 4.16.** Synthesis of BODIPY Acceptor.

**Scheme 4.17.** Synthesis of Di-styryl BODIPY and Mono-styryl BODIPY via Knoevenagel Condensation.

## Notations and Abbreviations

$\text{BF}_3 \cdot \text{OEt}_2$  - Boron trifluoride etherate

BODIPY – Boradiazaindacene,

BDT – Benzodithiophene

$\text{CHCl}_3$  - Chloroform

$\text{CDCl}_3$  - Deuterated chloroform

$\text{CH}_3\text{CN}$  – Acetonitrile

$^{13}\text{C}$ -NMR - Carbon-13 NMR

DDQ - 2,3-Dichloro-5,6-dicyano-1,4-benzoquinone

DCM – Dichloromethane

DMF – Dimethylformamide

DMSO – Dimethyl Sulfoxide

$^1\text{H}$ -NMR - Proton NMR

$\text{K}_2\text{CO}_3$  - Potassium Carbonate

LE state - Locally Excited state

$\text{MgSO}_4$  – Magnesium Sulphate

NMR - Nuclear magnetic resonance

$\text{NaHCO}_3$  - Sodium Bicarbonate

$\text{Na}_2\text{SO}_4$  - Sodium Sulphate

RT - Room Temperature

TICT - Twisted Intramolecular Charge Transfer

Tol - Toluene

THF - Tetrahydrofuran

TLC - Thin layer chromatography

UV-Vis - Ultraviolet Visible

## Abstract

Fluorescent molecular rotors (FMRs) based on electron donor acceptor systems showing twisted intramolecular charge transfer (TICT) upon photoexcitation are planned to be synthesized and investigated in this work. Such TICT based rotors show fluorescence properties that are sensitive to any change in its surrounding environment factors such as solvent temperature, polarity, viscosity, pH and so on. Most importantly, such FMRs can be very effectively used as temperature and viscosity sensors and can be utilized to study the temperature and viscosity of cellular microenvironments, a challenging problem to address otherwise. The hurdles faced during the establishment of ratiometric temperature/viscosity molecular probes for bio-imaging and sensing applications together with the propagation of red emitting rotors with photostability to match the tissue optical window and large Stokes shift for negligible autofluorescence. One of the most significant cellular organelle that often gets targeted for disease diagnosis is the mitochondria. The mitochondrial microenvironment parameters such as temperature, viscosity, pH often provide opportunities to investigate mitochondrial morphology and functions. Due to the presence of negative potential in the mitochondrial inner membrane, the positively charged cations get attracted towards it due to charge attraction hence increasing the mitochondria uptake of these molecules. The most commonly used cationic groups that target mitochondria are triphenylphosphonium (TPP), pyridinium salts and quaternary ammonium salts. In this project, red emitting donor-spacer-acceptor (D- $\pi$ -A) molecular rotors (**ADA-1** and **ADA-2**) based on TICT are planned to be synthesized in which BODIPY and BDT act as acceptor and donor respectively in a A-D-A configuration. The choice of an electron donating thiophene ( $\rho$ ) spacer will ensure the red or near infrared (NIR) emission of these rotors making them suitable for bio-imaging. These molecules will be functionalized with a mitochondria targeting group (quaternary salt of piperidine moiety) such that the emission sensitivity of these rotors to temperature and viscosity can be efficiently utilized to study and monitor mitochondrial microenvironments through ratiometric temperature sensing and viscosity sensing experiments. Owing to their multi-stimuli responsive emission behaviour, these rotors are thus expected to emerge as valuable fluorescent molecular rotor probes to monitor the levels of biologically relevant indicators in cells and organisms.

# Chapter 1

## Introduction

### 1.1. Fluorescent Molecular Rotors

Fluorescent molecular rotors are a growing section of pi-conjugated fluorophores (based on donor-acceptor systems) shows the occurrence of twisted intramolecular charge transfer (TICT) phenomenon upon photoexcitation where the molecule takes the path of twisted motion around the single bond leading to charge separation with the generation of a non planar relaxed perpendicular conformer in the excited state. This rotating activity around the bond linking the donor-acceptor molecule can be modulated by the surrounding environmental factors like solvent polarity, pH, temperature, viscosity and so on. The molecular rotors have been well established in various applications such as in microenvironment sensors for biological systems, organic photovoltaic devices, microfluidic applications, organic light emitting diodes, non-linear optics, polymer science and so on. The dual emission in 1,4-dimethylaminobenzonitrile was first reported by Grabowski, who demonstrated that the formation of both the Locally excited (LE) state and TICT excited state are the origin of the dual emissive behaviour where the shorter emission wavelength is observed through relaxation from the locally excited state and a longer emission wavelength characteristics through the relaxation from the TICT excited state known as the anomalous emission (Fig 1.1).<sup>1</sup>

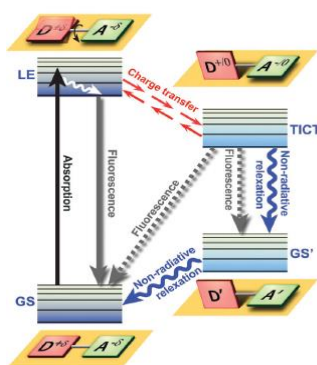


**Fig 1.1.** The general photophysical mechanism of Donor-Acceptor fluorophores undergoing TICT phenomenon.<sup>2</sup>

Due to this phenomenon dual fluorescence is observed. When these TICT active fluorophores are excited to the local excited state it remains in the same coplanar conformer as that of the ground state. Due to loss of energy through vibrational transition the electrons residing in the LE state jumps down to the more stable TICT state due to the conformational relaxation from a planar conformer to a non planar conformer (attaining a perpendicular conformer). The emission from the TICT excited state to the ground state gives rise to a lower energy emission which is less than the energy spent for normal absorption leading to a smaller energy gap resulting in an increase in the pseudo stoke shift <sup>3</sup> Generally the relaxation from the non planar perpendicular conformer is correlated with either an emission showing a red shift or non fluorescent relaxation which is determined by the structure of the molecule and the various deactivation pathways (radiative as well as non-radiative) taken up by the rotor during the twisting action.

In the TICT excited state of the rotor the twisting movement of the molecule gives rise to a pronounced charge separation state which leads to a surge in the dipole moment making the TICT state more polar. The existence of both the anomalous emission from the TICT excited state and the normal emission from the LE state is governed by the changes in the polarity of the solvent. The highly dipolar TICT state gets preferentially more stabilized in high polarity solvents (THF and acetonitrile) than the non polar ground state due to the generation of hydrogen bonds hence the formation rate of the TICT band increases. As a result of this stabilization of the TICT state in polar solvents, its energy decreases and accordingly the energy difference of the excited and the ground state also decreases leading to a bathochromic shift in the emission. LE band observed in the emission spectra of the rotor is insensitive to solvent polarity. Thus, in high polarity solvents, emission corresponding to TICT excited state is observed whereas in case of non- polar solvents such as hexane, methylcyclohexane (MCH) or toluene, only emission due to LE state is observed. Dual emission corresponding to both the LE and TICT excited states can be seen in medium-polarity solvents or binary mixtures of polar and non-polar solvents. The FMRs typically comprise of three components: an electron-donating component, an electron-accepting component and a  $\pi$ -conjugated electron-rich spacer (linking moiety) that facilitates charge separation from donor to acceptor (electron transfer) upon rotation in the photo excited state.<sup>4</sup> The representation of a typical structure of a molecular rotor is shown in Figure 1.2 along with some examples.<sup>5</sup>

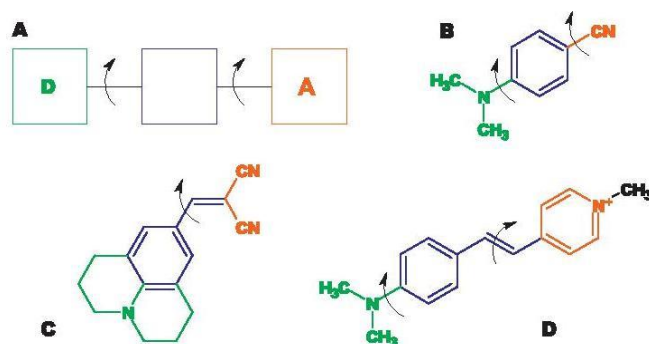


**Fig 1.2.** Illustrative structure of a TICT active rotor based on electron donor acceptor systems (A) displaying the electron donating moiety (green), the electron accepting moiety and the electron rich spacer (blue). Some basic examples are (B) 1,4-dimethylamino benzonitrile (DMABN), (C) 9-(dicyanovinyl) julolidine (DCVJ) and (D) p-(dimethylamino) stilbazolium (p-DASPMI).<sup>5</sup>

The viscosity of the solvent is another key parameter which influences the TICT band of the molecular rotors and the dynamics of LE-TICT transition. In viscous environment the TICT active rotor is unable to cross the potential energy barrier against the interconversion between LE to TICT state leading to the inhibition of conformational relaxation from the planar to non planar state, therefore it faces a hindrance in its intramolecular rotation.<sup>5</sup> Solvent polarity, pH and temperature also portray important roles in influencing the photophysical aspects of these TICT-active molecular rotors aside from viscosity. Solvatochromism is an important feature shown by these TICT molecules in which emission colour of the solution changes in solvents of varying polarity. It arises in consequence to permanent dipole moment present in the TICT state of the donor acceptor type of molecule. In case of negative solvatochromism, a hypsochromic shift in the emission signal is observed with decreasing solvent polarity since the excited state gets destabilized in non-polar solvents that will raise its energy bringing about an expansion in the band gap. On contrary for positive solvatochromism, emission spectra shifts to red with increasing solvent polarity as the molecule in its excited state possess a higher dipole moment than its ground state which is more stable in polar solvents. A bathochromic shift in the emission spectra is noticed while increasing the polarity in case of TICT excited state since being high dipolar in nature it tends to get stable in polar solvents.



## **1.2. Working Principle of TICT based Fluorescence Molecular Rotors as Viscosity and Temperature sensors**

Viscosity-sensitive FMRs have emerged as indispensable tools with high efficiency in the areas of biosensing, biomedical applications and bioimaging by tracking the microviscosity of specific sub-cellular organelles, detection of chemical analytes and important biomolecules due to its fast response and high specificity. Any changes in the cellular viscosity might affect the normal working conditions of the cell since it helps in maintaining all the diffusion mediated processes occurring inside the cell leading to its abnormal functioning as well as its high susceptibility to pathological attacks therefore monitoring of spatially resolved intracellular microviscosity is required to gain knowledge regarding the situation of the cell in a normal condition as well as in a diseased condition. In all biological systems, both flow and viscosity portrays a key aspect from the microscopic to the elementary level.<sup>6</sup> The major disadvantage encountered in case of measuring viscosity is its need of a dreary and time consuming evaluation technique, costly equipments with a limited sample length to work upon. Measurement of viscosity and temperature is an irrelevant exercise on a macroscopic level but on a microscopic level (for instance atmospheric aerosols or live cells) investigating their distribution becomes quite demanding as it is required to retrieve data in a smaller scale resolution in the range of micrometers with the addition of intracellular microenvironment being highly inhomogeneous making it all together difficult to sense local environment.<sup>6</sup> This is where the fluorescence environmental sensitive probes comes into the picture where it can be pursued as a beneficial approach to measure viscosity as well as temperature constraints on the microscale in an effective manner.<sup>7</sup> With the induction of changes in the microenvromental viscosity, the fluorescence signal of these sensitive probes varies accordingly. A representative diagram of the working principle of viscosity based fluorescence sensor is explained in fig 1.3 below.

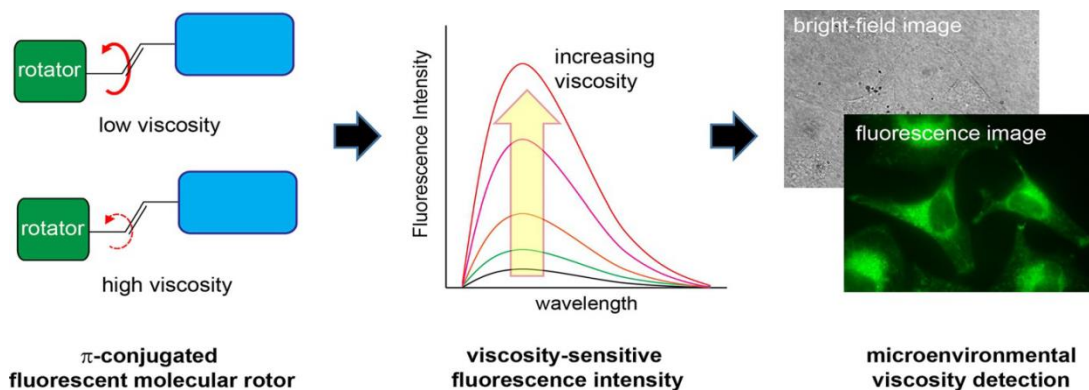


**Fig 1.3.** Schematic outline behind the operation of viscosity based TICT active molecular rotors.<sup>3</sup>

For molecular rotors sensitive to viscosity only fluorescence from the LE state is apparent including the absence of the TICT emission band. It is because the twisting action of the rotors is hampered progressively under a viscous solvent environment leading to the inhibition of conformational relaxation from the coplanar structure to the perpendicular non planar structural state.<sup>3</sup> Therefore amplification in the fluorescence intensity is achieved which transpires as a result of the emission happening through the LE state to the ground state. The rapid accelerating twisting motion of the donor and acceptor components around a single bond promotes non-radiative deactivation of the excitation energy culminating in the dampening of the emission intensity in a solvent with less viscosity. So increment in the viscosity of the surrounding medium induces an enhancement in the fluorescence (FI) intensity with a swift growth in the fluorescence lifetime and quantum yield of the rotor owing to the restricted motion of the rotor stretching the duration of its presence in the initial fluorescence state.<sup>8</sup> For the improved capacity of the TICT active viscosity sensor requirement of elevated measurements of fluorescence contrast and fluorescence efficiency is necessary. In case of temperature sensors, with elevated temperature constraints, reduction in the fluorescence intensity is attained owing to faster molecular rotations leading to non-radiative decay of energy. But sometimes during high temperature conditions, it is enough to administer the required activation energy to jump across the potential energy barricade for the back interconversion from the stable TICT excited state to the LE state causing increment in the emission intensity (LE state becomes more populated).<sup>9</sup>

### 1.3. Study of properties and examples of different types of sensors

The introduction of meso phenyl ring in the structural core of BODIPY (boron-dipyrromethene) based FMRs imparts a viscosity responsive ability considering the active fast rotations of the meso-phenyl ring substituents and its high fluorescence quantum yield. The main concept is that the fluorescence activity of such meso-phenyl functionalized boron-dipyrromethene (BODIPY) derivatives are modulated by the action of non-radiative deactivation pathway taken up by the molecule owing to its twisting movements along the single bond coupling the meso-carbon of the BODIPY scaffold and the phenyl ring. There is an upsurge in the fluorescence output of these BODIPY based rotors due to the suppression in the twisting motion of the phenyl ring or the BODIPY rotor in the presence of high viscosity environment. In a reduced viscosity neighborhood, quenching in the fluorescence intensity is noted due to the occurrence of rapid molecular rotations resulting in the enhancement of the non-radiative deactivation phenomenon. The addition of a chemical substitution on the BODIPY compartment or the presence of various substituents on the phenyl group controls the several attributes associated with the BODIPY associated molecular rotors.<sup>10</sup> A list of meso functionalized BODIPY based molecular rotor with variation in the substituent groups were studied in fig 1.4. The twisting action of the meso-phenyl moiety across the C-C single bond is sterically hindered due to the existence of different chemical substituents at the ortho position of the phenyl moiety or at the 1st and 7th position of the BODIPY compartment.<sup>11</sup>

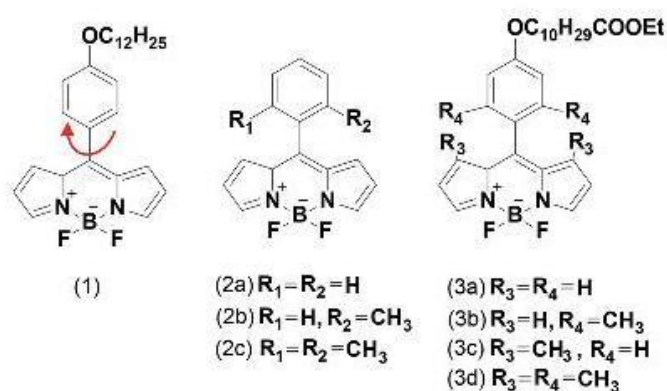


**Fig 1.4.** Examples of BODIPY based FMRs with chemically functionalized meso-phenyl ring in the presence of different substituents.<sup>3</sup>

There are two methods that can subdue the uncertainties correlated with the measurement of the fluorescence output of a FMR such as fluctuations in concentration, irregular illumination,

turbidity in the sample and variation of excitation laser power. The first criteria is established on the notion of ratiometric detection. Haidekker and his group narrated about a ratiometric rotor comprising of amalonitrile-type viscosity sensitive molecular rotor 2-cyano-3-(4-dimethylaminophenyl)acrylic acid methyl ester (CMAM) covalently coupled to a 7-methoxycoumarin-3-carboxylic acid (MCCA) operating as a viscosity insensitive reference dye via an aliphatic spacer (Figure 1.5).<sup>12</sup> The two characteristic peaks observed in the fluorescent spectra of the ratiometric rotor discussed above is proportioned in such a manner that the fractions of these two peaks is affected by its surrounding viscosity as the fluorescence activity of the reference component of the fluorophore shows no change in the intensity. This kind of fluorescence response cancels out the overall effect of the concentration of the ratiometric dye on it. The second criteria that increases the chances of getting a response independent of concentration is via the exploitation of the fluorescence lifetime of fluorophores.

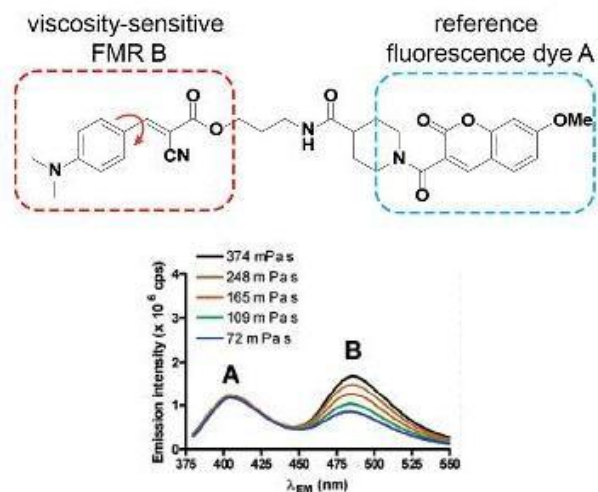


**Fig 1.5.** The structural diagram and emission characteristics (in increasing viscosity) of a viscosity responsive rotor linked to a non-responsive reference rotor (CMAM-MCAA) based on ratiometric detection approach.<sup>12</sup>

During the conditions when there is a lack of quenching and aggregation, the fluorescence lifetime acting as an ideal parameter provides us with the accurate observation of environmental microviscosity independent from the effect of outside parameters such as concentration, optical setups, detection ranges and additional calibration sets. Cao et al conceived a TICT active temperature responsive chromophore (Figure 1.6) that represents the quenching of emission

wavelength and intensity with elevated temperature considering the aiding of conformational conversion to a TICT state which relies on the effect of temperature upon excitation.<sup>13</sup>

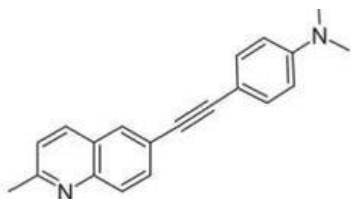


**Fig 1.6.** Fluorescence molecular rotor with displaying temperature responsive attributes.<sup>14</sup>

The property of dual responsive character corresponding to the variations in both viscosity as well as temperature is manifested in various fluorophores are not attractive since it provides us with inconclusive results regarding the fact if the alteration in the emission output is due to the modification of the surrounding viscosity or temperature parameters. For example in case of the TICT active chromophore BODIPY C<sub>10</sub> (Fig 1.7), it was seen that in the presence of variable temperature lifetime parameter of such rotor was same in solvents of equivalent bulk viscosity.<sup>11</sup> Hence this rotor does not have any ambiguity regarding the output of the fluorescence signal or show dual sensitivity to both temperature and viscosity. It signifies that BODIPY C<sub>10</sub> is only sensitive to modifications in the viscosity of the mixtures while having minimal intrinsic responsiveness to temperature.<sup>6</sup>

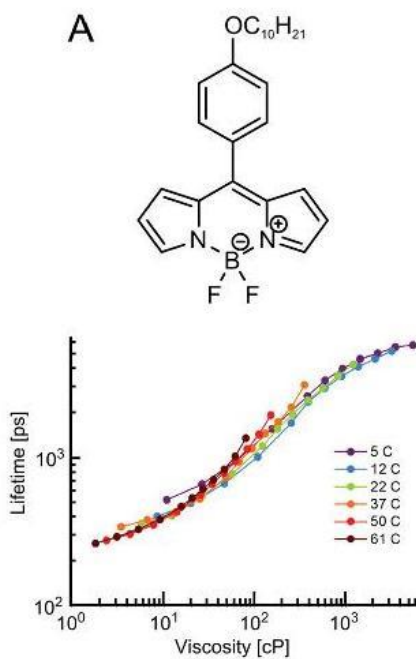


**Fig 1.7.** Lifetime evaluation graph of BODIPY C<sub>10</sub> at different viscosity and temperature conditions.<sup>11</sup>

## **1.4. Application of Fluorescence molecular rotors in sensing and imaging within specific organelles**

In order to measure macroscopic viscosity fundamental approaches were adopted such as capillary viscometers, equipments tracking the downward action of the ball and evaluation of the guidelines of the rotating elements.<sup>7</sup> But these tactics are not applicable for live biological systems as huge sampling data is necessary and organelle specific microviscosity measurements is almost next to impossible if these techniques are considered for its tracking. Therefore, fluorescence molecular rotors can be clearly needed for this goal owing to the pronounced spatiotemporal sensitivity of their emission to viscosity as mentioned before. Organelles behave as functional compartments of the cell confined within their own lipid bilayer.<sup>15</sup> The most important organelles of the cell are nucleus, golgi body, mitochondria, endoplasmic reticulum, lysosomes etc. where all of them perform cellular functions of equal weightage. For example, the nucleus handles the encoding of genetic material and its expression, mitochondria are accountable for energy supply for the production of ATP, and lysosomes decompose macromolecules for cell reprocessing.<sup>16</sup> Two parameters are responsible for the healthy functioning of the cell which is the presence of certain useful biological species with the addition of a convenient micro-environmental state to function within. Therefore, interruption in the equilibrium of such species or micro-environmental state causes malfunctioning of the organelle, inducing various ranges of disordered conditions inside the cell. It is crucial to monitor for particular biological species and the local microenvironment region inside important cellular organelles to afford explicit information on their portrayal in the physiopathology of organelles. The advantage of stimuli responsive fluorescent probes have been studied to address on the effect of the microenvironmental factors owing to the fact that the emissive characteristics of fluorescent probes gets aided or hampered by the local environmental changes.<sup>5</sup> A miscellaneous batch of organelle-staining fluorescent probes are readily accessible which cooperates in biological research of intracellular transport, substrate degradation, respiration, detoxification, and mitosis including others.<sup>17</sup>

### **1.4.1. Mitochondrial-targeting group functionalized probes**

Mitochondria is sausage shaped, double membrane organelle incorporated in the cytoplasm of relatively all living cells, recognized for its activity including aerobic metabolism, cellular

signaling pathways, cellular differentiation, apoptosis (cell death), as well as perpetuating the role of the cell growth and cycle. When mitochondria is in a dysfunctional state, malfunctioning in the cell is triggered from the disorganized energy supply which arises ending to the collapse of the respiratory chain for the generation of ATP which might lead as a crucial reason behind the deterioration of the cell causing an array of human diseases.<sup>18</sup> It is significantly useful to gain awareness regarding the physiological functioning and the associated mitochondrial deformation conditions with the intention of visualizing the dynamic cellular processes going on in the mitochondria via the use of the accessible tools like mitochondrial localized probes which can target mitochondria in a biological setting. Proton gradient is maintained as negative membrane potential (-180 mV) across the mitochondrial inner membrane which gets produced during the process of cellular respiration and is considered as one of the essential attributes of mitochondria.<sup>19</sup> The purpose of mitochondrial localized probes is dependent on this inner membrane negative potential which will attract the TICT active molecular rotors functionalized with a lipophilic cation towards itself due to electrostatic interaction, increasing the chances of mitochondrial uptake of these molecules. The two most widely used approaches facilitating mitochondrial targeting capacity are:

- (a) Incorporation of a mitochondria targeting cation into the fluorophore system and (b) desired lipophilicity (important factor since it is necessary to be soluble in the mitochondrial matrix). The lipophilicity of the cations in addition to the Delocalized Positive Charge (DLCs) is capable of infiltrating the hydrophobic boundaries of the mitochondrial membrane and matrix respectively. The well-established criterion requires the covalent binding of the positively charged mitochondrial targeting group and the reaction site to the neutral chromophore scaffold (Fig 1.8A).<sup>20</sup> The examples of some cationic groups to target mitochondria are pyridinium salts, triphenylphosphonium (TPP) and quaternary ammonium salts. From these lipophilic cations, TPP is adopted extensively as a mitochondrial targeting functional group by virtue of its geometry, delocalized cationic  $\pi$ -system, rigidity, hydrophilic character and stability of TPP moiety in biological environment. Another criteria that generally requires the adoption of the chromophore as a DLC entity for localization in mitochondria is covalently bonded with the reaction site (Fig 1.8 B).<sup>21</sup> The application of xanthene (rhodamine 123) and cyanine based (JC-1) dyes acting as fluorescent lipophilic cations are developed in mitochondrial

staining.<sup>22</sup> Consequently, these fluorescent probes allow tracking of the modification in physical parameters such as temperature and viscosity taking place inside the mitochondria due to fluctuation in the levels of viscosity, metal ions, reactive oxygen/nitrogen species, thiols, pH, *etc.*, by FLIM. This shows that the application of such small molecule fluorescent probes functionalized with a mitochondria targeting moiety is instrumental in detecting variation in the levels of micro-environmental components like temperature, pH, viscosity and chemical species like thiols, oxygen/nitrogen species, metal ions and the monitoring of such alteration is possible via FLIM (Fluorescence Lifetime Imaging Microscopy). It also gives us some scope to feature mitochondrial abundance, localization and activity, as well as to produce observations regarding the effects of chemical agents that vary mitochondrial functions.<sup>23</sup>

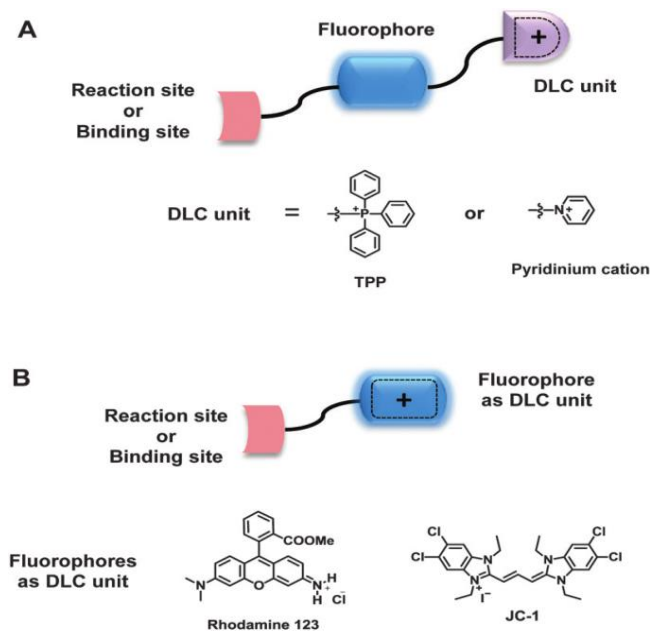


**Fig 1.8.** General illustration of two well known pathways for the layout of a mitochondrial targeting functionalized chromophore.<sup>21</sup>

But for the long term precise measurements of the effect of the alteration in the physical parameters, the presence of mitochondrial targeting group in the fluorophore is not enough due to the dynamic nature of the mitochondria. That means the authenticity of this charge attraction is not guaranteed since during any pathological or diseased conditions the potential across the mitochondria will be minimal hence prolonging the presence of these molecules inside the mitochondria will be difficult causing its out-flux from the mitochondria. Hence tracking of



unhealthy mitochondria is quite improbable during the loss of membrane potential therefore to in order to escape this situation, inclusion of the possibility of immobilization needs to be considered. Introduction of anchoring group which facilitates the immobilization of fluorophore onto the mitochondrial membrane was carried out in the positively charged MitoTracker series<sup>24</sup> comprising of an extra benzyl chloride moiety (anchoring unit) (Fluorophore 3 in Fig 1.9).

The benzyl chloride moiety attached to the fluorophore covalently bonds itself to the protein sulfhydryls present in the mitochondrial inner membrane via nucleophilic substitution mechanism. So even after the potential drops the fluorescence tracker will remain immobilized onto the mitochondrial membrane hence making the tracking process go smoothly for long periods of time.<sup>24</sup>

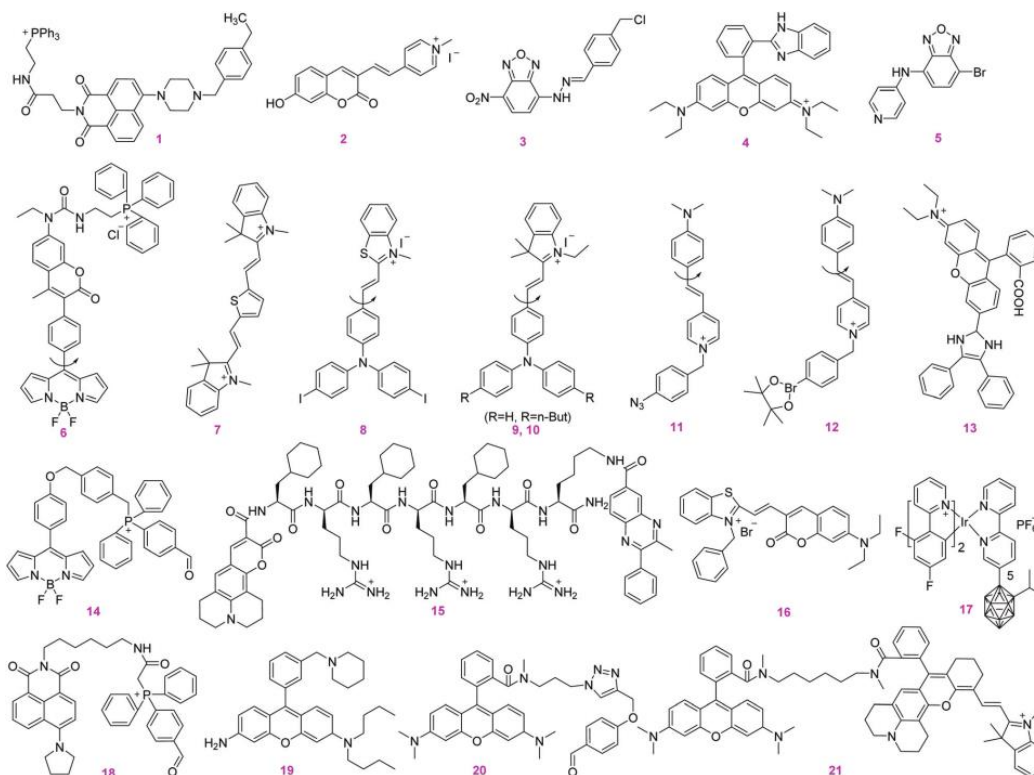


**Fig 1.9.** Fundamental examples of positively charged mitochondrial specific group functionalized fluorophore.<sup>25</sup>

For accurate monitoring of mitochondrial viscosity BODIPY rotor Vis A was introduced by Xiao in 2017 to prove the stable co-localization of the viscosity rotor during extreme conditions.<sup>26</sup> It depicts that it is equipped with a cationic TPP group for mitochondrial targeting and an aldehyde group that can adhere itself onto the mitochondrial inner membrane via imine bond formation between the aldehyde group and the amine group attached to the proteins of the inner membrane showing immobilizable property (Fig 1.10).

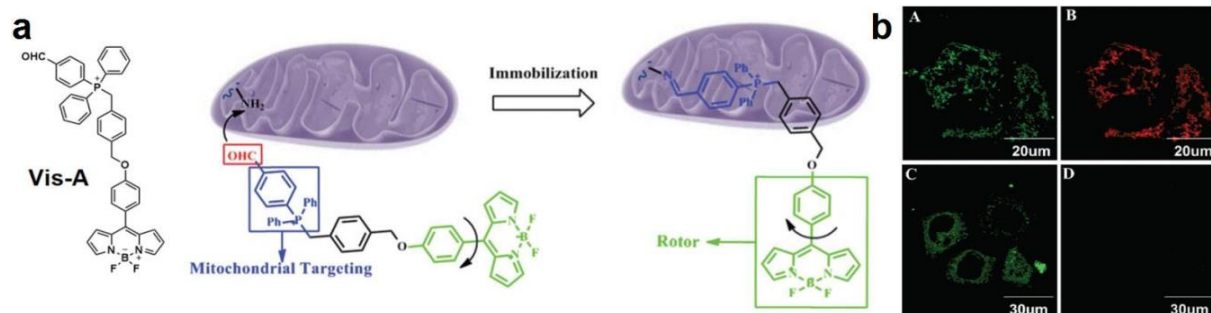


**Fig 1.10.** (A) BODIPY Vis A rotor showing the working principle of immobilization onto the mitochondria. (B) The bio-imaging of BODIPY Vis A viscosity rotor and Mitotracker DeepRed inside mitochondria in the absence and presence of formaldehyde.<sup>25</sup>

Another experiment was conducted in which the live cells were stained with BODIPY Vis A rotor MitoTracker DeepRed fluorophore (reference compound) and the effect of formaldehyde on the fluorescence output was monitored. From Fig 1.10 (B) it was observed that Vis A rotor with an anchoring group (aldehyde group) was able to show sustainable emission even under the presence of formaldehyde whereas for MitoTracker DeepRed without an anchoring group, depletion of the fluorescence was observed after the addition of formaldehyde exhibiting stable co-localization property of the Vis A rotor.

#### 1.4.2. Lysosome localized fluorescent molecules

Lysosomal viscosity gives knowledge regarding the activity and condition associated with lysosome since it keeps altering its position, morphologies, and constituents. Cellular debris or needless macromolecules are dumped in the cell's recycling centre called the lysosome where the needless macromolecules get converted into miniscule molecules for later usage by the cell. During lysosomal malfunction, macromolecules do not disintegrate while it keeps on getting collected inside the lysosome leading to the modifications of lysosomal viscosity due to the local

alteration in surrounding environment. Lyso-V was the first viscosity dependent TICT active molecular rotor, functionalized with a lysosome targeting group that can be used for the real time analysis<sup>27</sup> of its local microenvironment variation which could then provide valuable information in reference to any lysosome based dysfunctions. It consists of a morpholine unit acting as a lysosome targeting group which is connected to the BODIPY scaffold (Fig 1.11).<sup>28</sup> Sensitivity to viscosity arises from the unrestricted rotation across the C-C single bond linking the BODIPY unit to the meso- phenyl ring. Since the pK<sub>a</sub> value of the morpholine is in 5-6 range it can only get protonated in lysosomes which has a pH range from 4.5-5.5 irrespective of other organelles and cytosol.<sup>29</sup> Morpholine moiety in Lyso V with its moderate alkaline behavior and its lysosome active fluorescence properties tends to be favorable for its explicit localization in acidic lysosomes. The BODIPY fluorescence is diminished via photoinduced electron transfer (PET) due to the introduction of electron-rich morpholine moiety therefore, the background fluorescence will be imperceptible for the remnant of Lyso-V present outside the lysosomes.<sup>30</sup> However, inside the lysosomes, protonation of the morpholine moiety takes place which cannot be used as an electron donating unit for PET anymore therefore only the Lyso-V molecules that are retained inside the lysosomes are able to show fluorescence.

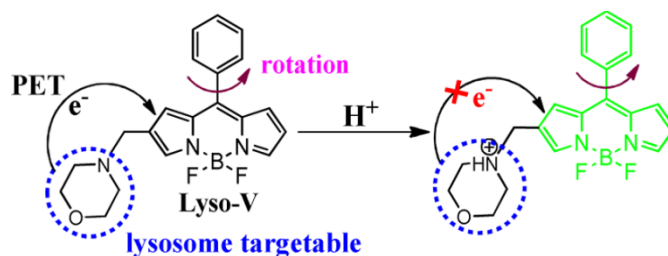


**Fig 1.11.** General mechanism behind the working of the Lyso-V molecular rotor.<sup>28</sup>

### 1.4.3. Nucleus targeting functionalized Probes

The nucleus functions as the central head of the cellular organization where it cultivates the purity of the genes and regulates the movement of the cell by monitoring genetic expression. The fundamental basis of genes is deoxyribonucleic acid (DNA), and the first stage to genetic expression is transcription by ribonucleic acids (RNA). DEAT-TO-3 (diethylamino)butyl) is a TO-3 derivative (1-ethyl-4-((1E,3Z)-3-(3-methylbenzo[d]thiazol-2(3H)-ylidene)prop-1-en-1-yl)quinolin-1-iumiodide) (Fig 1.12) with low energy excitation and emission ( $\lambda_{\text{abs}}(\text{DNA}) = 626$  nm and  $\lambda_{\text{em}}(\text{DNA}) = 649$  nm) that was endowed for live-cell DNA imaging and quantification.<sup>15</sup>

DEAB-TO-3 derives a large fluorescence amplification upon coupling with the native DNA and demonstrates a specific preference towards double-stranded DNA rather than for single stranded RNA. DEAB-TO-3 is favorable for the tracking of nucleus-specific imaging, highly sensitive DNA in-vitro and DNA quantification in-vivo.<sup>31</sup>

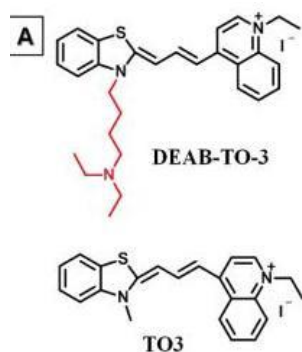


**Fig 1.12.** Structures of DEAB-TO-3 and TO-3 Nucleus Localized Probe.<sup>15</sup>

### 1.5. Motivation behind the project

The hurdles faced during the establishment of ratiometric temperature/viscosity molecular probes for bio-imaging and sensing applications together with the propagation of red emitting rotors with photostability to match the tissue optical window and large Stokes shift for negligible autofluorescence.<sup>32</sup> Recently our group described the subsistence of regioisomeric D-A (Donor-Acceptor) fluorescent molecular rotors, acceptor–donor–acceptor (A–D–A) triads built upon a BODIPY acceptor and a benzodithiophene donors which are electronically decoupled by a para phenyl spacer or a meta-phenyl spacer (Fig 1.13).<sup>33</sup> The response of regioisomerism (para- vs. meta- connectivity of phenyl spacer to D and A) on the viscosity along with temperature sensing characteristics, TICT and AIE (Aggregated induced emission) aspects of these compounds were investigated.

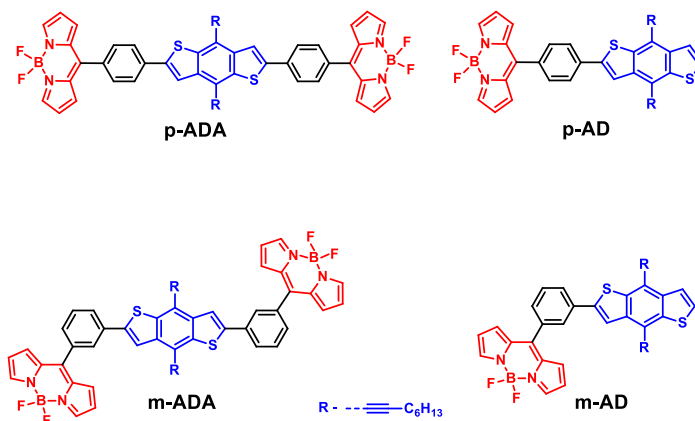


**Fig 1.13.** Representative molecular design of regioisomeric dyads *p-AD* and *m-AD* and ADA triads *m-ADA*, *p-ADA* prepared and studied in this work.<sup>33</sup>

Three primary peak characteristics were manifested in all compounds analogous to a wide peak encompassing ca. 360–380 nm similar to a prolonged conjugation of the phenyl sub-unit along BDT and BDT (ca. 312–322 nm), and BODIPY (ca. 504 nm) (Figure 1.14). Peaks about 312–322 nm is analogous to BDT  $\pi$ - $\pi^*$  transition and the peaks encompassing 504 nm is analogous to BODIPY  $S_0$ - $S_1$  transition. The stoke shift of *p-ADA* was found to be 150 nm which was 44 nm lower in value with respect to *p-ADA* displaying a stoke shift of 194 nm.<sup>33</sup>

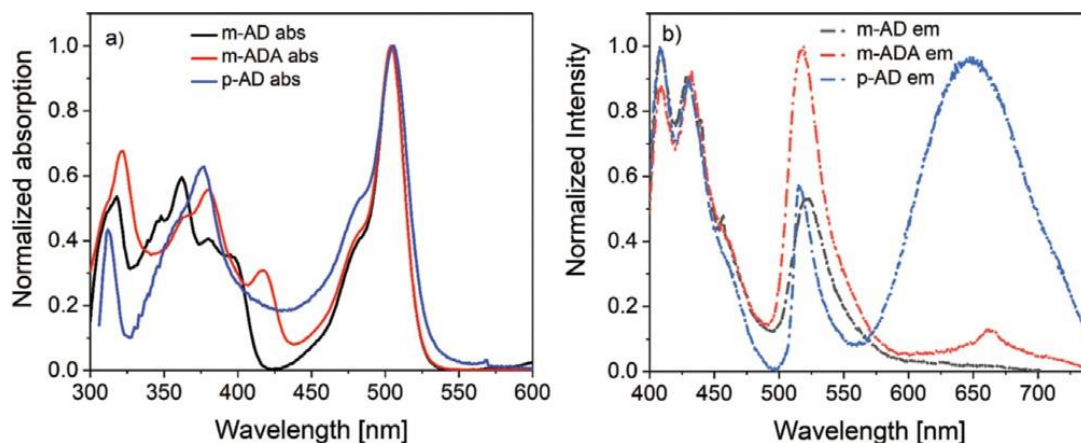


**Fig 1.14.** Correlation of absorption spectra for *m-ADA*, *p-AD* and *m-AD* in chloroform ( $c=10^{-5}$  M); b) Normalized emission data for *p-AD*, *m-ADA* and *m-AD* in  $\text{CHCl}_3$  ( $c=10^{-5}$  M) upon exciting at 377 nm, 380 nm and 362 nm, in conjunction.<sup>33</sup>

Viscosity-dependent emission spectra were characterized in a series of ratios of MeOH and glycerol for triad *m-ADA* and dyads *p-AD* and *m-AD* to achieve the repercussion of viscosity on the conformations of these given molecules in its excited condition. There was an enhancement in the fluorescence output with rising solvent viscosity adopting a binary mixture containing glycerol/methanol solution for each and every compound. Since the intramolecular rotation gets abolished in the viscous environment, it influences the non-radiative decay channels and thus the TICT band was missing in case of both dyads *p-AD* and *m-AD* (Figure 1.15) and in triads' *m-*

ADA and *p*-ADA. Solvent polarity held no role in the characterization of these compounds and the blue shift observed was mainly associated with the rigidification of the molecular geometry.<sup>33</sup>

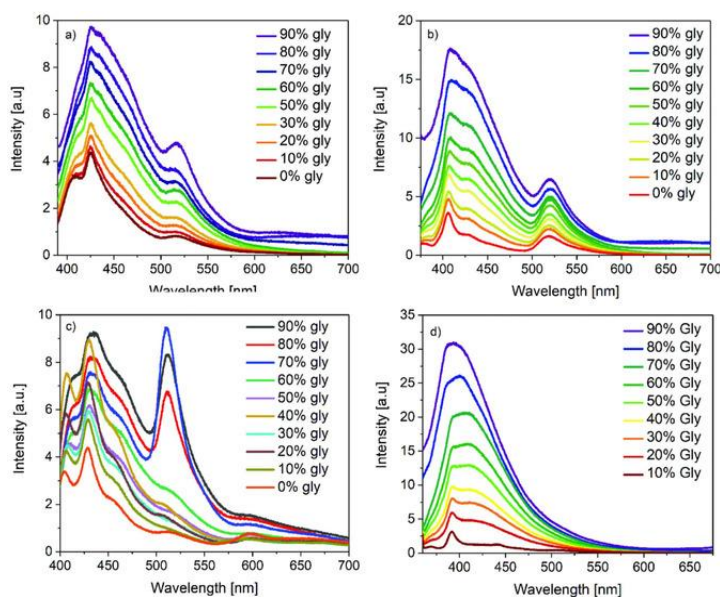


**Fig 1.15.** Emission spectra of dyads a) *p*-AD and b) *m*-AD, and triads c) *p*-ADA and d) *m*-ADA in solution various viscosities.

## 1.6. Our Objective

The motive of the present thesis is to utilize the above discussed molecular design principle utilizing BDT and BODIPY portraying as donor and acceptor respectively in a A-D-A configuration and functionalize these molecules with mitochondria targeting groups such that the emission sensitivity of these rotors to temperature and viscosity can be efficiently utilized to study and monitor mitochondrial microenvironments. The molecular design adopted in the project is depicted in fig 1.16.

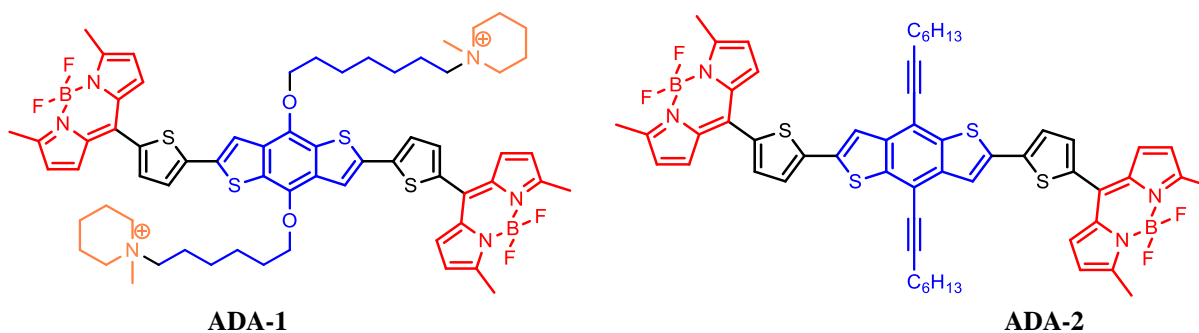


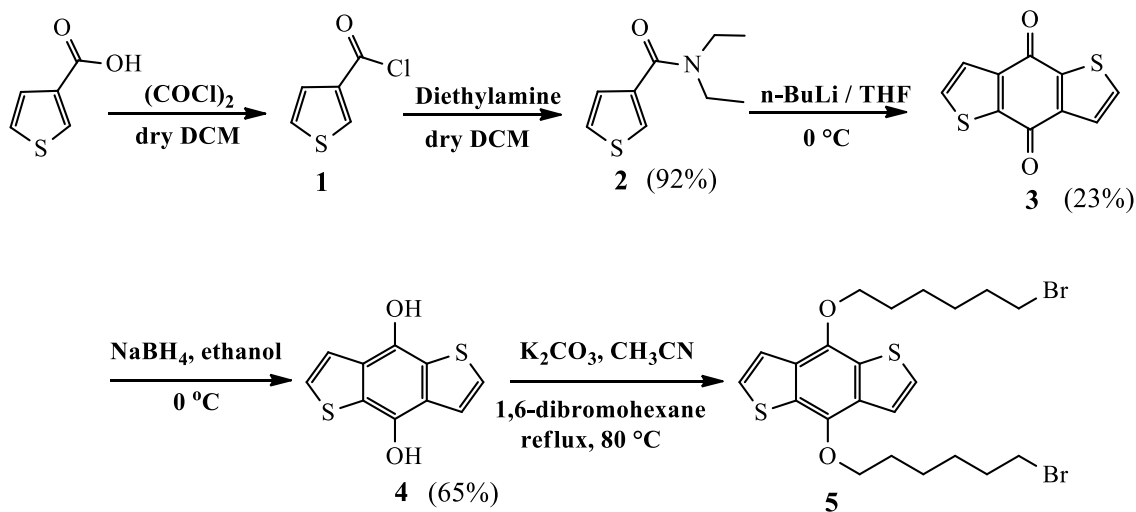
**Fig 1.16.** Molecular design adopted in this project.

As shown in Fig 1.16, **ADA-1** comprises of BDT and BODIPY portraying as donor and acceptor moieties with the presence of piperidine group in the BDT moiety which can be quaternized in the final step and then these positively charged quaternary ammonium ion can help in mitochondria targetability. Owing to the strong electron donating character of thiophene spacer attached to the acceptor part and the presence of only two methyl groups in BODIPY core, this rotor molecule will most likely emit in the NIR or red region with a higher Stokes shift than our earlier reported rotors.<sup>34</sup> On the other hand, **ADA-2** is a spectroscopic reference compound in which the mitochondria targeting group is absent. These two molecules can be used for various bio-imaging and bio-sensing applications.

## Chapter 2

### Results and Discussion

The project commenced with the synthesis of (*N,N*-diethyl)thiophenecarboxylamide (**2**) compound in Scheme 2.1 which was performed starting from thiophene-3-carboxylic acid, oxalyl chloride and then the carbonyl (in-situ formation of acid chloride) was converted to corresponding amide using diethylamine. Subsequently, (*N,N*-diethyl)thiophenecarboxylamide (**2**) compound was treated with *n*-BuLi at 0 °C to give Benzo[1,2-*b*:4,5-*b'*]dithiophene-4,8-dione (BDT-dione) (**3**) as shown in Scheme 2.1. For the synthesis of the donor part 4,8-Bis[(6-bromohexyl)oxy]benzo[1,2-*b*:4,5-*b'*]dithiophene (**5**) was synthesized initiating from compound 4,8-Bis(hydroxy)benzo[1,2-*b*:4,5-*b'*]dithiophene (BDT-diol) (**4**) and compound **3** as shown in Schemes 2.1 and 2.2. The main challenges faced while synthesizing compound **5** from BDT diol was that it had to be subjected to 5-6 cycles of freeze-pump-thaw degassing to remove the dissolved oxygen present in the solution to facilitate the forward reaction and to suppress BuLi inactivation due to the presence of moisture.



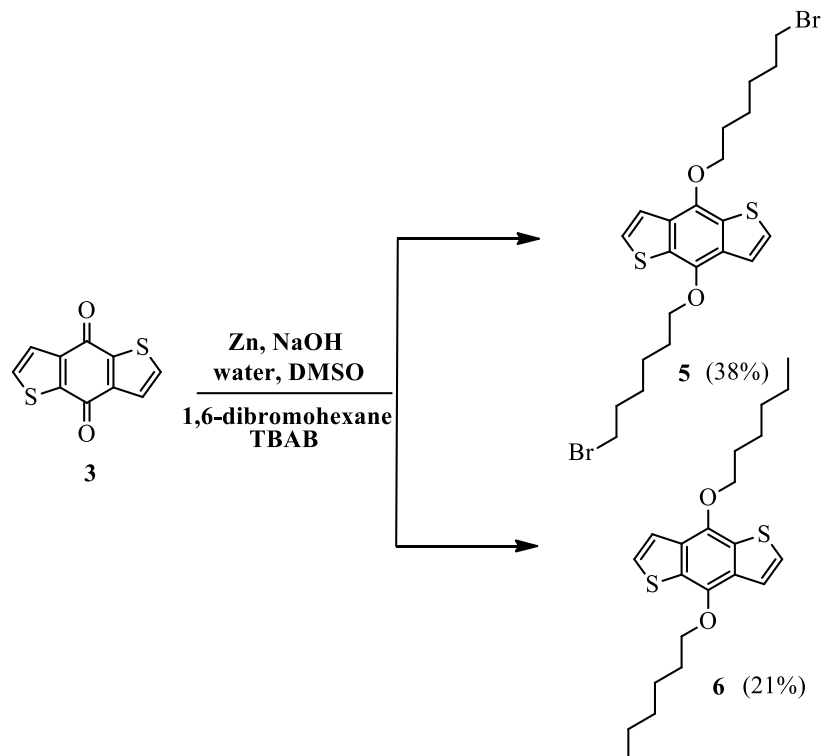
**Scheme 2.1.** Synthesis of 4,8-Bis[(6-bromohexyl)oxy]benzo[1,2-*b*:4,5-*b'*]dithiophene (**5**) from BDT-diol (**4**).

It was observed that the BDT-diol (**4**) compound got converted back into BDT-dione compound (**3**) in the presence of oxygen which led to failed reaction since the alkylating reagents used in



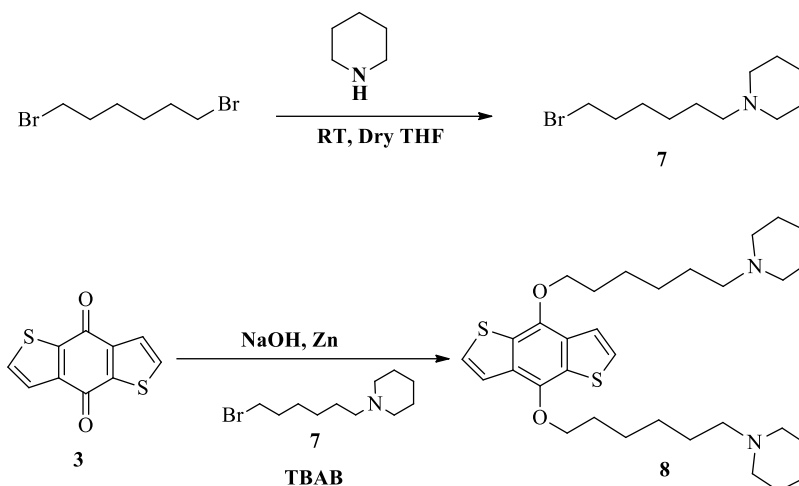
Scheme 2.1 would react only with the hydroxyl groups and not the keto groups. Even after several freeze-pump-thaw cycles, and inert atmosphere conditions, presence of starting compound was ascertained and the product formed was not the desired one as identified from the NMR spectra, hence the reaction failed.

In case of synthesis of compound **5** from BDT dione (**3**) (Scheme 2.2), many trial reactions were conducted using different equivalents of NaOH, zinc and also using different solvents such as only water, DMSO and water mixture, ethanol and water mixture and so on. It was found that if zinc was introduced in two portions, once before the addition of NaOH and another portion after the addition of 1,6-dibromohexane, two products were formed i.e., 4,8-bis(hexyloxy)benzo[1,2-b:4,5-b']dithiophene (**6**) and 4,8-Bis[(6-bromohexyl)oxy]benzo[1,2-b:4,5-b']dithiophene (**5**). So, with increase in the equivalents of NaOH and with addition of zinc in two portions, there was a higher chance of formation of 8-bis(hexyloxy)benzo[1,2-b:4,5-b']dithiophene (**6**) instead of 4,8-Bis[(6-bromohexyl)oxy]benzo[1,2-b:4,5-b']dithiophene (**5**). The conclusion is that after the formation of 4,8-Bis[(6-bromohexyl)oxy]benzo[1,2-b:4,5-b']dithiophene (**5**), it underwent dehalogenation to form the 4,8-bis(hexyloxy)benzo[1,2-b:4,5-b']dithiophene (**6**) due to the addition of high equivalent (eq.) of strong base NaOH. Therefore the eq. of NaOH was decreased and Zn was supplemented only once to get the desired product 4,8-Bis[(6-bromohexyl)oxy]benzo[1,2-b:4,5-b']dithiophene (**5**). However, the yield of the reaction was 37 % and the reaction led to many side products with close  $R_f$  values so it was quite time consuming to separate the desired product in its pure form and characterize it via  $^1\text{H}$  NMR. The original thought was to conduct stannylation reaction on 4,8-Bis[(6-bromohexyl)oxy]benzo[1,2-b:4,5-b']dithiophene (**5**) using  $\text{SnMe}_3\text{Cl}$ , however, the terminal bromo groups being labile functionalities might not withstand the addition of strong base  $n\text{-BuLi}$  and may undergo elimination and it was envisaged that the  $\text{BuLi}$  may preferentially attack the terminal  $\text{CH}_2\text{Br}$  of alkyl chains instead of attacking the aromatic protons (at 2-position) next to the sulphur atoms in the BDT core of **5**.



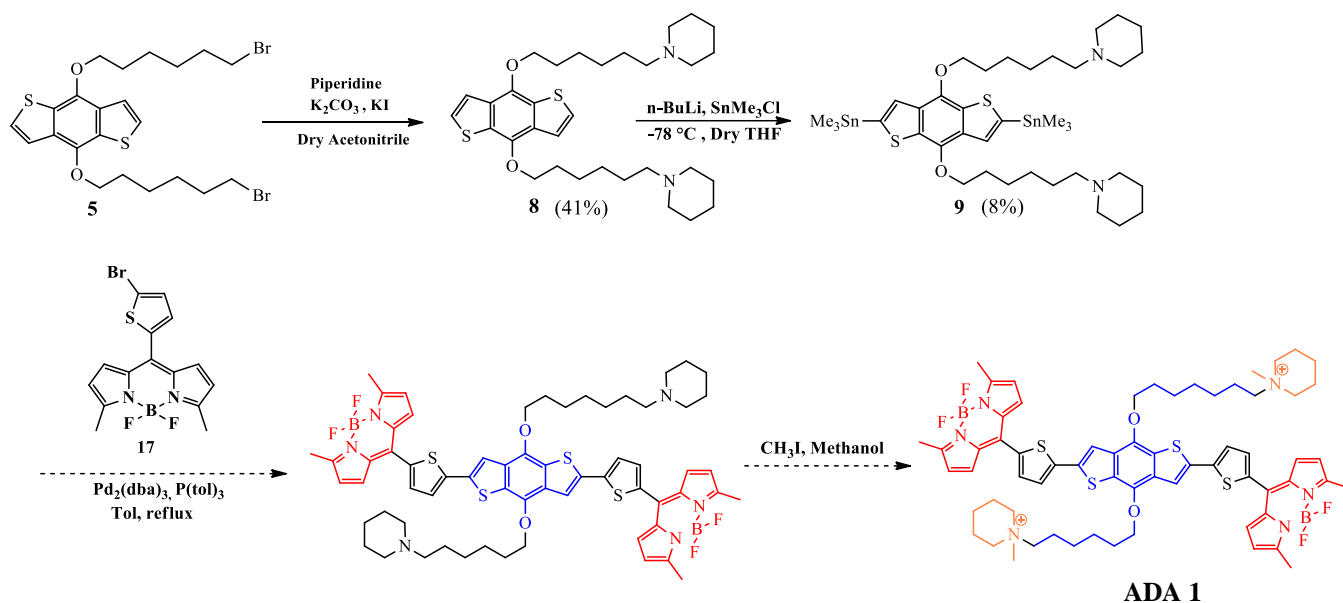
**Scheme 2.2.** Synthesis of 4,8-Bis[(6-bromohexyl)oxy]benzo[1,2-b:4,5-b']dithiophene from BDT-dione (3).

Thus, it was essential to substitute the bromo group with a more stable functionality that can not only withstand the *n*-BuLi attack but can also be converted as a positively charged cationic group later on in the synthesis scheme. Therefore, piperidine group was incorporated in the design to replace the Br at the end of alkyl chain so that it fulfills the criteria of withstanding BuLi reaction as well as its post modification into a cationic group. Keeping this idea in mind, firstly the synthesis of the chain 1-(6-bromohexyl)piperidine (7) was done by reacting piperidine with 1,6-dibromohexane. Then the synthesis of 4,8-Bis(6-(1-hexyloxy)piperidine)benzo[1,2-b:4,5-b']dithiophene (8) was carried out using 1-(6-bromohexyl)piperidine (7) chain and the BDT-dione compound (3) but this also failed since the NMR of the compound was not appropriate. (Scheme 2.3)



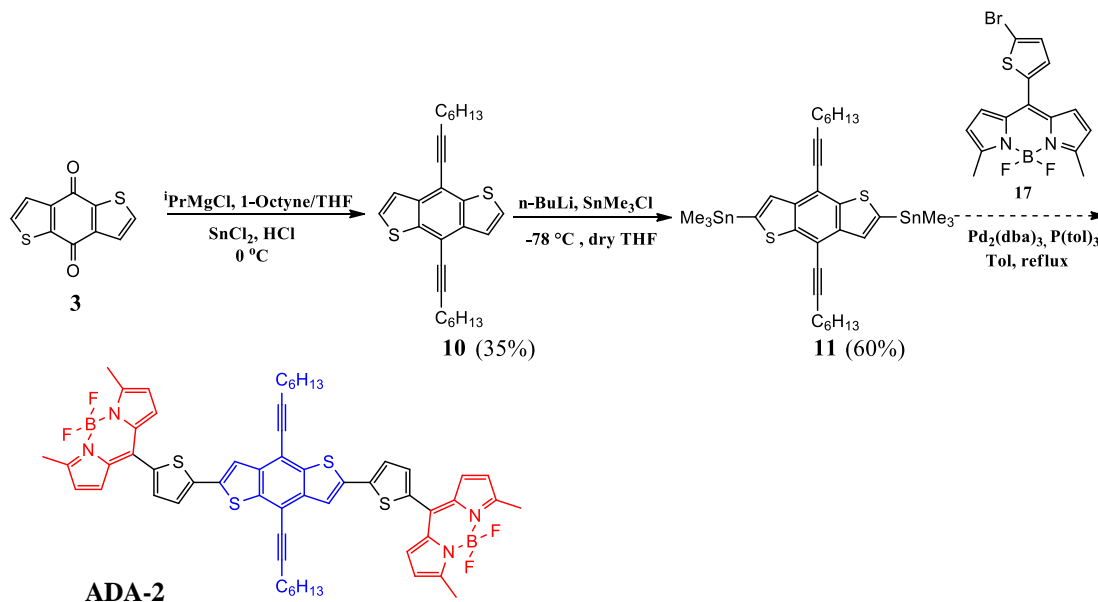
**Scheme 2.3.** Synthesis of 4,8-Bis(6-(1-hexyloxy)piperidine)benzo[1,2-*b*:4,5-*b'*]dithiophene (8) from BDT-dione (3).

Then another route for the synthesis of 4,8-Bis(6-(1-hexyloxy)piperidine)benzo[1,2-*b*:4,5-*b'*]dithiophene (8) was tried using the 4,8-Bis[(6-bromohexyl)oxy]benzo[1,2-*b*:4,5-*b'*]dithiophene (5) compound by simple substitution reaction which led to the formation of a very polar compound. The main challenge faced here was its poor solubility in various solvents making it only partially miscible in solvents such as methanol, THF and acetonitrile. Usually for the stannylation reaction, an aprotic solvent with a very low freezing point (FP) like THF is used such that the solvent is maintained in its liquid state at cryogenic temperature (-78 °C) where the *n*-BuLi can function optimally. However, since the solubility of compound **12** in THF was poor, the use of other aprotic solvents like DMF (FP = -62 °C) and acetonitrile (FP= -41 °C) were also explored. But the reactions in the solvents dry THF and dry DMF didn't lead to an effective result since there was a lot of starting material present in the reaction medium. In case of reaction in dry acetonitrile, formation of a less polar compound with respect to starting material was observed which needed to be identified with the NMR. If the 1,1'-[4,8-bis[(6-(1-hexyloxy)piperidino)benzo[1,2-*b*:4,5-*b'*]dithiophene-2,6-diyl]bis[1,1,1-trimethyl-stannate (9) is formed then it can be coupled to the acceptor part (thiophene functionalized BODIPY, 17) via Stille coupling after which the piperidine moiety can be quarternized using methyl iodide and the final product **ADA-1** can be formed (as shown in Scheme 2.4).



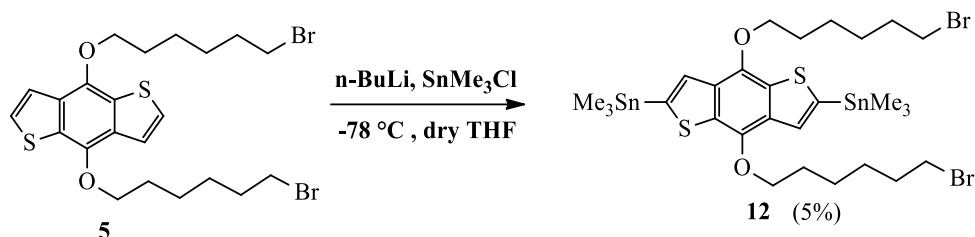
**Scheme 2.4.** Synthetic scheme for the synthesis of **ADA-1** compound.

For the synthesis of **ADA-2** compound, first grignard reaction of BDT-dione (**3**) was performed using  $i\text{PrMgCl}$ , 1-octyne and  $\text{SnCl}_2/\text{HCl}$  to obtain 4,8-Di(oct-1-yn-1-yl)benzo[1,2-b:4,5-b']dithiophene (**10**) and subsequently stannylation of compound **10** was performed using  $n\text{-BuLi}$  and  $\text{SnMe}_3\text{Cl}$ . The resultant compound (4,8-di(oct-1-yn-1-yl)benzo[1,2-b:4,5-b']dithiophene-2,6-diyl) bis(trimethylstannane) (**11**) will be subjected to Stille coupling with BODIPY in presence of  $\text{Pd}_2(\text{dba})_3$  and  $\text{P}(\text{tol})_3$  as catalysts (Scheme 2.5) and dry toluene as the solvent.



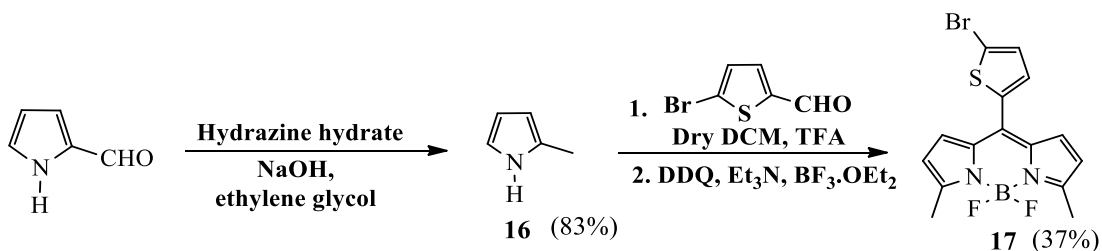
**Scheme 2.5.** Schematic diagram for the Synthesis of ADA-2 compound (reference compound).

The stannylation reaction with compound (**5**) was also performed by adding less eq. of n-BuLi at first in which only starting material was observed (Scheme 2.6). Subsequently, n-BuLi was used in excess amount which led to the formation of two products (above starting material) with the existence of unreacted starting material. The characterization of the two products is yet to be done via  $^1\text{H}$  NMR in order to draw any conclusion.



**Scheme 2.6.** Synthesis of 1,1'-[4,8-bis[(6-bromohexyl)oxy]benzo[1,2-b:4,5-b']dithiophene-2,6-diyl]bis[1,1,1-trimethyl-stannate].

For the acceptor part, the synthesis of BODIPY (**17**) was started as shown in Scheme 2.7 which was performed using 2-methylpyrrole, 2,3-Dichloro-5,6-dicyano-1,4-benzoquinone (DDQ) as oxidizing agent and boron insertion was carried out using Et<sub>3</sub>N and BF<sub>3</sub>·(OEt)<sub>2</sub>. The challenges faced while synthesizing BODIPY was in its purification where many by-products were obtained and the unreacted DDQ needed to be removed carefully by a flash column prior to the column chromatographic purification of **17**.



**Scheme 2.7.** Synthesis of 8-(2-bromothiophen-5-yl)-3,5-dimethyl-4,4-difluoro-4-bora-3a,4a-diaza-s-indacene (BODIPY) (**17**).

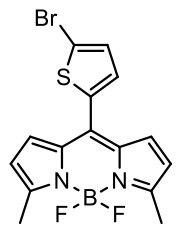
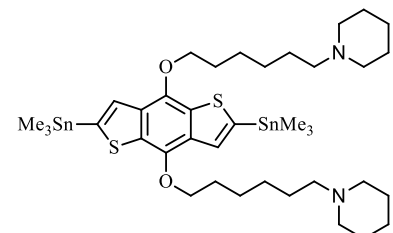
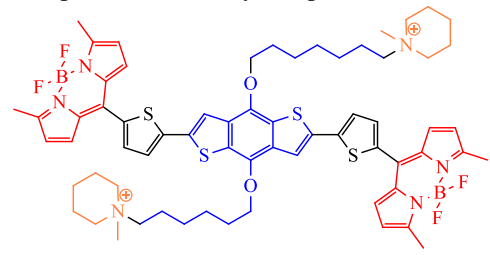
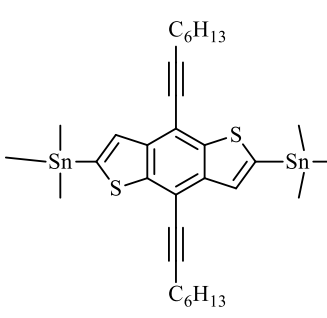
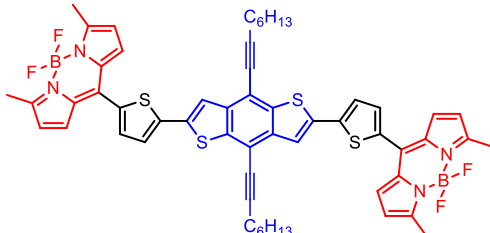
## Chapter 3

### Summary and Outlook

This thesis focuses upon the synthesis of twisted intra-molecular electron transfer (TICT) fluorescent molecular rotor compounds **ADA-1** and **ADA-2** (Table 3.1) which are based on BODIPY dye portraying as electron donor and benzodithiophene (BDT) portraying as electron acceptor. The concept of utilizing these chromophores in the design of molecular rotors are based on our recent work and ongoing work that justify their suitability as efficient rotors having adjustable emission properties in the red and near-infrared (NIR) region along with pronounced responsiveness to external stimuli such as temperature, viscosity, polarity, and so on. The planned rotor **ADA-1** has specific cellular organelle targetability i.e., mitochondria targetability owing to the presence of cationic side chains that can bind effectively to the mitochondria. Thus, this rotor can play a significant role as a multifunctional fluorescent probe for detecting mitochondrial microenvironmental parameters such as viscosity, temperature, pH etc, bio-sensing as well as in bio-imaging. Rotor **ADA-2** on the other hand lacks the mitochondria targeting cationic group and therefore will serve as a spectroscopic reference compound that can be used to understand the response of temperature, polarity of the solvent and viscosity on the emission output. The synthesis and characterization of **ADA-1** and **ADA-2** were not yet finished since the synthetic procedures had significant challenges but the syntheses are intended to be continued in the group beyond this thesis. The syntheses of donor and acceptor precursor molecules were successfully carried out and the donor molecules are yet to be characterized via  $^1\text{H}$  NMR and  $^{13}\text{C}$  NMR. Due to the lengthy synthetic strategies and other difficulties such as solubility issues and fewer yields, there were challenges in the preparation and purification of donor molecule functionalized with the piperidine moiety. Several structural modifications were adopted accordingly and the different synthetic schemes to prepare either a donor or acceptor molecule attached to mitochondria targeting group have been discussed in detail in the experimental section but most of them were unsuccessful. The O-alkylation of BDT-dione with 1,6-dibromohexane was challenging since the reaction resulted in many side products with negligible  $R_f$  difference that made separation of these compounds almost impossible by column chromatography and significantly decreased the yield of the desired compounds. These kind of molecular rotors such as **ADA-1** with an organelle targeting group is quite useful in monitoring

the viscosity/ temperature variations in mitochondria can be used as viscosity and temperature sensors and can facilitate our understanding of essential mitochondria-related cellular events. Furthermore, both rotors **ADA-1** with targeting group and **ADA-2** without the organelle targeting group are envisaged to exhibit red or NIR emission characteristics and as a result of low autofluorescence and high penetration depth, will be well-suited for bio-imaging applications. Owing to their multi-stimuli responsive emission behavior, these rotors are thus expected emerge as valuable fluorescent molecular rotor probes to monitor the levels of biologically relevant indicators in cells and organisms. In the future endeavors of our research group, immobilization of mitochondrial/other cell organelle targeting probes will be taken up in which the molecular rotors will not only have a specific organelle targeting ability but will also have an anchoring group which will adhere covalently to the mitochondrial inner membrane and will block these molecules from leaving the mitochondrial environment during any pathological attacks hence improving its tracking and monitoring abilities. Finally, synthetic modifications by introducing water soluble side chains in the design are also planned that can ensure enhanced cellular uptake of these molecular rotors.

**Table 3.1.** Summary of the work.

|              |   | <b>ACCEPTOR</b>   |
|--------------|---|---|
|              |   |    |
| <b>DONOR</b> |    | <p style="text-align: center;"><b>ADA-1</b></p> <ul style="list-style-type: none"> <li>• Mitochondrial targeting group present.</li> <li>• Compound is polar and less soluble.</li> <li>• Expected red or NIR emission.</li> <li>• Emission tunability with solvent polarity, temperature, viscosity and pH.</li> </ul>  |
|              |  | <p style="text-align: center;"><b>ADA-2</b></p> <ul style="list-style-type: none"> <li>• Absence of mitochondrial targeting group.</li> <li>• Compound is less polar and soluble.</li> <li>• Expected red or NIR emission.</li> <li>• Emission tunability with solvent polarity, temperature, viscosity.</li> </ul>     |



# Chapter 4

## Experimental Section

### General Information:

#### 4.1. Materials

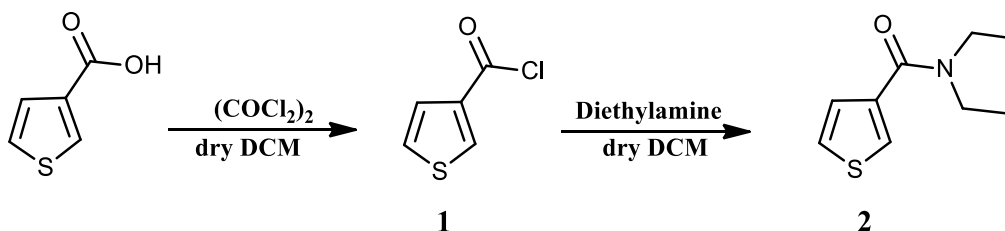
All reagents and solvents were acquired from Sigma Aldrich, Merck, and Himedia. Solvents such as dichloromethane (DCM) were distilled using standard distillation setup, where toluene was dried using Mbraun MB-SPS solvent drying unit. Tetrahydrofuran (THF) was dried over sodium/benzophenone and distilled before utilization. DCM was dried over phosphorus pentoxide and distilled before utilization. Dimethylformamide (DMF) gets dried over calcium sulphate and distilled under reduced pressure prior to use. Acetonitrile gets dried over calcium hydride and distilled before utilization. Drying of Toluene was also processed over sodium/benzophenone and distilled before utilization. Silica gel of mesh size 60-120 was adopted for column chromatography. Solvents used for column chromatography and extraction (such as hexane, DCM, chloroform and ethyl acetate) were directly utilized without any further distillation. Reactions were followed via thin layer chromatography (TLC) plates on silica gel and visualized under UV lamp (254 and 365 nm).

#### 4.2. Measurements

The recording of  $^1\text{H}$  and  $^{13}\text{C}$  NMR spectra was carried out on a 400 MHz BrukerBiospinAvance III FT-NMR spectrometer with TMS as standard at room temperature. The solvents used were  $\text{CDCl}_3$  and  $\text{DMSO-d}_6$  and MeOD. Column chromatography was implemented with silica gel of mesh size 100-200.

#### 4.3. Synthesis

##### 4.3.1. Synthesis of (*N,N*-diethyl)thiophenecarboxylamide

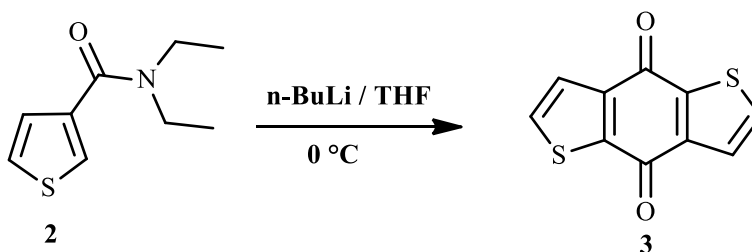


**Scheme 4.1.** Synthesis of (*N,N*-diethyl)thiophenecarboxylamide.

Dissolution of Thiophene-3-carboxylic acid (2g, 15.6057 mmol) in 15 mL of DCM was introduced in a round-bottomed (RB) flask equipped with guard tube filled with CaCl<sub>2</sub>. The addition of 7.92 g (62.4228 mmol) of oxalyl chloride was processed in a drop-wise manner while the solution was kept for cooling on an ice bath. The reaction mixture was kept for stirring overnight at ambient temperature. The removal of exorbitant quantities of oxalyl chloride was done underneath vacuum. A dissolution of the intermediary acyl chloride compound (**1**) in 15 mL of dry DCM was then introduced to the solution in a dropwise manner which has the presence of diethylamine 3.2 g (43.7517 mmol) in 30 mL of dry DCM in a two necked RB equipped with a CaCl<sub>2</sub> guard tube while kept for cooling on an ice bath. The stirring of the reaction mixture was carried out for 3 h at room temperature and washed with water and extricated with 40 mL DCM twice. The collection of organic fraction was done and dried using anhydrous sodium sulphate, solvent gets evaporated by rotary evaporator and purified by silica gel column chromatography using ethyl acetate/hexane (30/70 v/v) mixture as eluent. Pure compound (**2**) was collected as an oily liquid with a yield of~ 92%.

<sup>1</sup>H NMR (400MHz, CDCl<sub>3</sub>): δ (ppm) = 7.47-7.32 (m, 1H), 7.31 (d, *J* = 4Hz, 1H), 7.26 (d, *J* = 4 Hz, 1 H), 3.52-3.37 (m, 4 H), 1.24-1.19 (d, *J* = 20 Hz, 6 H).

**4.3.2. Synthesis of Benzo[1,2-b:4,5-b']dithiophene-4,8-dione**



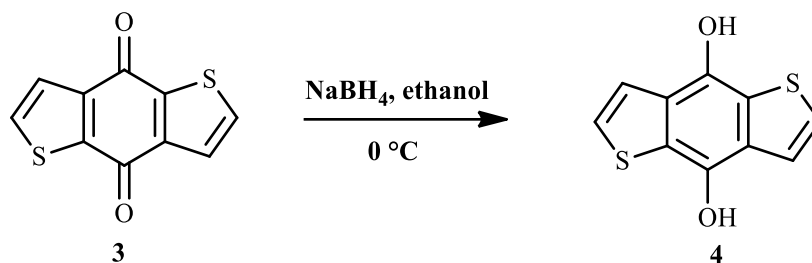
**Scheme 4.2.** Synthesis of Benzo[1,2-b:4,5-b']dithiophene-4,8-dione (BDT-dione) (**3**).

Compound **2** (1 g, 5.455 mmol) gets dissolved in distilled THF. Under nitrogen environment conditions the addition of 6.11 mL of *n*-BuLi (1.6M in hexane) was done in a drop-wise style in to the solution containing compound **2** while it was getting cooled to 0 °C. The solution was kept for stirring for 3 h at room temperature and after which was then drained into a beaker which consists of ice-water. Formation of yellowish precipitate was seen immediately and the mixture

gets to stir overnight. The precipitate formed was filtered with the help of Buchner funnel apparatus and washed with water, methanol and hexane successively and kept for drying under vacuum. A yellow solid **3** was obtained as the product with ~ 23 % yield.

**<sup>1</sup>H NMR (400MHz, CDCl<sub>3</sub>):**  $\delta$  (ppm) = 7.69 (d,  $J$  = 4 Hz, 2 H), 7.65 (d,  $J$  = 4 Hz, 2 H).

#### 4.3.3. Synthesis of 4,8-Bis(hydroxy)benzo[1,2-b:4,5-b']dithiophene



**Scheme 4.3.** Synthesis of 4,8-Bis(hydroxy)benzo[1,2-b:4,5-b']dithiophene(BDT diol) (**4**).

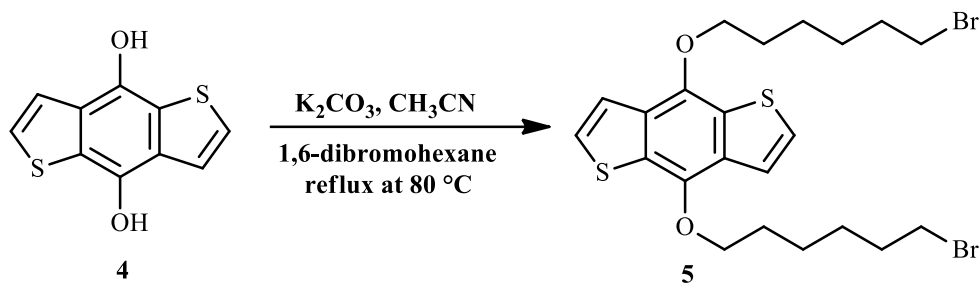
BDT-dione (**3**) (100 mg, 0.454 mmol) and ethanol was dissolved in a schlenk tube and sodium borohydride (NaBH<sub>4</sub>) (68.69 mg, 1.816 mmol) in ethanol was dissolved in another schlenk tube. Then they were subjected to 5 cycles of freeze-pump-thaw degassing in order to discard the dissolved oxygen from the solution. Subsequently, the solution of NaBH<sub>4</sub> was introduced in a drop-wise fashion at 0 °C to a solution of **3** and ethanol under nitrogen atmospheric conditions. The reaction gets allowed to stir for 5 h at room temperature. The reaction mixture was then neutralized using 1M HCl and filtered via vacuum filtration to yield dark green powder including a yield of ~ 65%.

**<sup>1</sup>H NMR (400MHz, DMSO):**  $\delta$  (ppm) = 9.80 (s, 2 H), 7.62 (d,  $J$  = 8 Hz, 2 H), 7.56 (d,  $J$  = 4 Hz, 2 H).

#### 4.3.4. Synthesis of 4,8-Bis[(6-bromohexyl)oxy]benzo[1,2-b:4,5-b']dithiophene

Different procedures were used for the optimization of the reaction and to synthesize this compound in high yield.

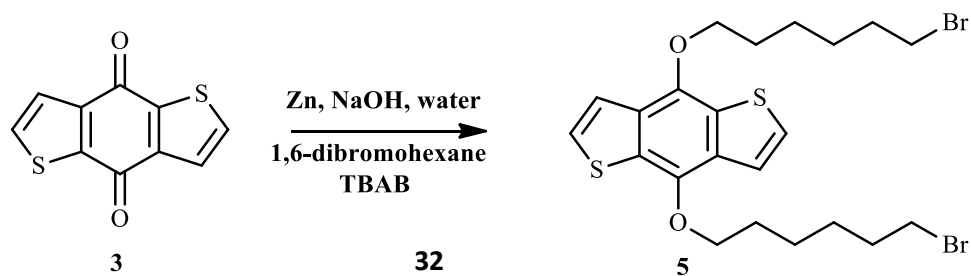
## Procedure 1



**Scheme 4.4.1.** Synthesis of 4,8-Bis[(6-bromohexyl)oxy]benzo[1,2-b:4,5-b']dithiophene (5) from BDT-diol (4).

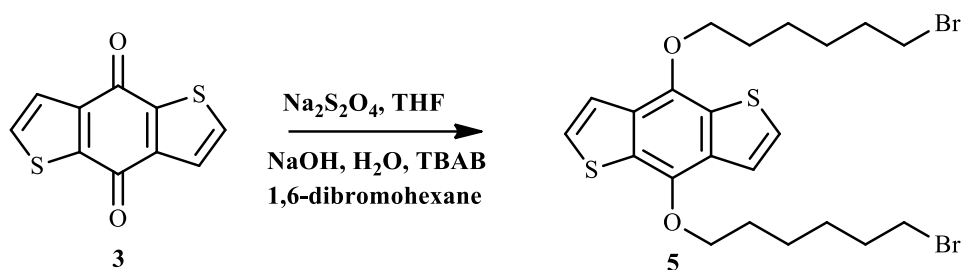
4,8-Bis(hydroxy)benzo[1,2-b:4,5-b']dithiophene (4) (50 mg, 0.227 mmol) was solubilized in acetonitrile (15 mL) in one schlenk tube and 1,6-dibromohexane (118.3 mg, 0.485 mmol) dissolved in acetonitrile (10 mL) in another schlenk tube, both were put through 6 freeze-pump-thaw degassing cycles. Subsequently,  $K_2CO_3$  (313.72 mg, 2.27 mmol) was put in a 2-neck 50 mL RB flask and in the presence of nitrogen atmosphere, the BDT diol (4) acetonitrile solution was added. Following this, 1,6-dibromohexane-acetonitrile solution was added in that RB flask containing  $K_2CO_3$  and the solution colour converted to dark bluish. The solution with reaction mixture was kept for refluxing for 48 h at  $80\text{-}85\text{ }^\circ\text{C}$ . After the culmination of the reaction, workup was performed using DCM ( $4 \times 10\text{ mL}$ ) and water ( $3 \times 10\text{ mL}$ ) and the washing of the organic layer was done with saturated brine solution several times and the collection of organic layers was done and kept for drying over  $Na_2SO_4$  with the removal of solvent under vacuum in a rotary evaporator. In the TLC, two spots were visible where the lower spot corresponds to the starting material BDT. The purification of crude product was done via column chromatography using ethyl acetate/hexane (1/9 v/v) mixture as eluent. While purifying the compound by column chromatography, one of the upper spots converted into 2 new spots which were collected, however, the NMR of these fractions did not show the expected product peaks, hence the reaction failed.

## Procedure 2



**Scheme 4.4.2.** Synthesis of BDT-dibromo-O-alkylated product (**5**) from BDT-dione (**3**) using water as the solvent. In the solution of **3** (100 mg, 0.454 mmol), zinc dust (89.09 mg, 1.362 mmol) and water (10 mL) gets added to it and is stirred at RT after which NaOH (352 mg) gets added directly and the reaction solution gets to reflux at 90 °C for 2 h. The cooling of mixture to room temperature was accomplished followed by the addition of 1-bromohexane (0.22 mL, 1.452 mmol) and tetra-n-butylammonium bromide (TBAB) (20 mg, 0.04 mmol) in a sequential manner. The stirring of reaction mixture was kept at 80 °C for 12 h. After checking TLC, the crude mixture only had starting material.

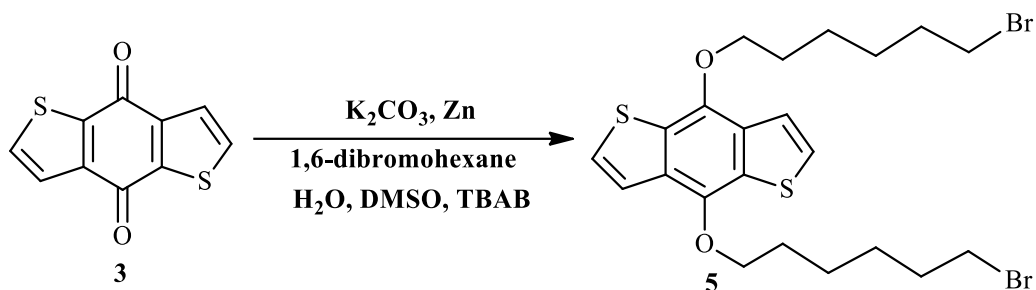
### Procedure 3



**Scheme 4.4.3.** Synthesis of BDT-dibromo-O-alkylated product (**5**) from BDT-dione using water and THF as the solvent and using sodium dithionite as the reducing agent.

Under nitrogen atmosphere, benzo[1,2-b:4,5-b']dithiophene-4,8-dione (**3**) (100 mg, 0.454 mmol),  $\text{Na}_2\text{S}_2\text{O}_4$  (237.37 mg, 1.36 mmol), and tetrabutylammonium bromide (319.14 mg, 0.99 mmol) in water (12 mL) were well mixed for 10 min after which the addition of dry THF (16 mL) was performed, along with the addition of NaOH (272.05 mg, 680 mmol). Under nitrogen atmosphere conditions the mixture gets to stir for 2 h at room temperature. Subsequently, the addition of 1,6-dibromohexane (0.205 mL, 1.35 mmol) was performed followed by the overnight stirring of the mixture at 80 °C. Checking the TLC indicated the presence of only reactant in the reaction mixture.

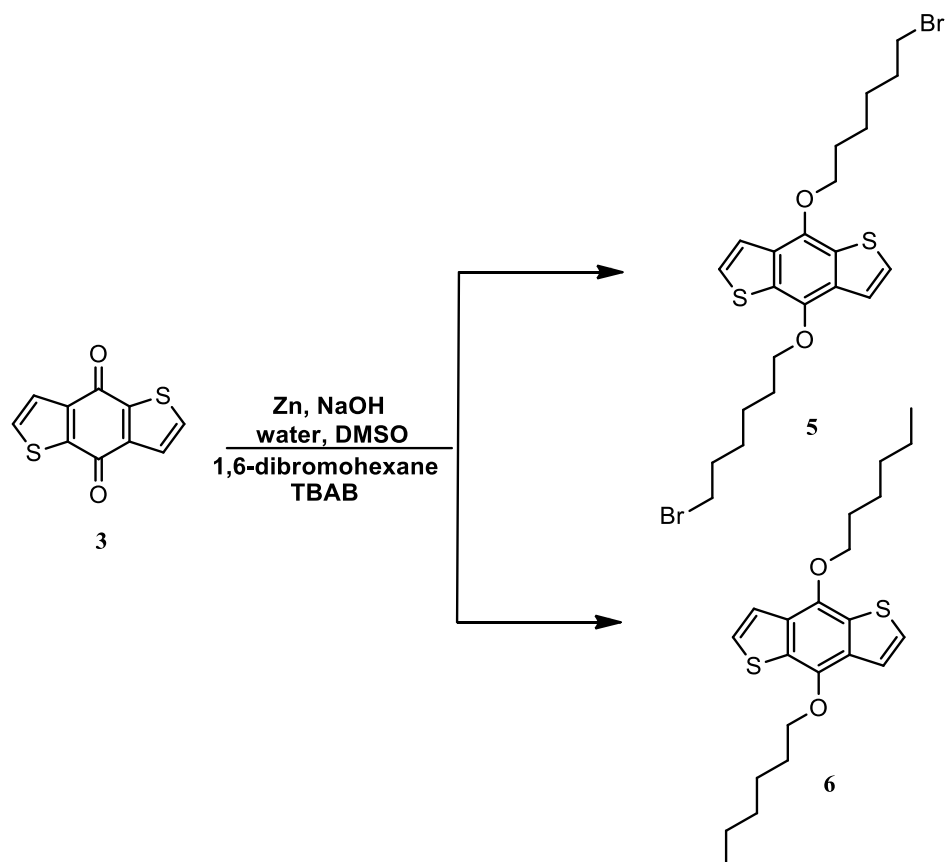
### Procedure 4



**Scheme 4.4.4.** Synthesis of BDT-dibromo-O-alkylated product (**5**) from compound **3** using water and DMSO as the solvent and using  $\text{K}_2\text{CO}_3$  as a mild base.

Benzo[1,2-b:4,5-b']dithiophene-4,8-dione (**3**) (50 mg, 0.227 mmol), zinc powder (35 mg, 0.522 mmol), 10 mL of water, and 4 mL of DMSO (dimethyl sulfoxide) were introduced into a 50 mL RB flask followed by addition of  $\text{K}_2\text{CO}_3$  (470 mg, 3.40 mmol) into the reaction mixture. The mixture was well stirred under nitrogen atmosphere and heated to reflux for 2 h. Subsequently, 1,6-dibromohexane (155.06 mg, 0.635 mmol) and a catalytic amount of TBAB were introduced into the flask. After refluxing for 2 h, the reaction mixture colour changed from deep red to greenish yellow. During the refluxing action for additional 16 h, the colour of the reaction mixture gradually changed from yellow to orange. After the completion of the reaction it was drained into cold water ( $6 \times 10$  mL) and extricated with 40 mL of diethyl ether thrice. The combined ether layers were dried over anhydrous  $\text{Na}_2\text{SO}_4$  and was then the removal of solvent was performed under vacuum in a rotary evaporator. TLC was checked after workup and only starting material was present.

#### Procedure 5



**Scheme 4.4.5.** Synthesis of BDT-dibromo-O-alkylated product (**5**) from BDT-dione (**3**) using water and ethanol as the solvent and using NaOH as a strong base.

Benzo[1,2-b:4,5-b']dithiophene-4,8-dione (**3**) (50 mg, 0.227 mmol) and zinc dust (44.52 mg, 0.681 mmol) were mixed together in water (10 mL) which was kept for stirring at RT and then NaOH (1.7 g, 17% NaOH) was introduced directly to the solution in the presence of nitrogen environment. Subsequently, DMSO (4 mL) was introduced to the reaction mixture and the color changed from yellow to dark red and then it was refluxed at 80 °C for 2 h. The cooling of mixture to room temperature conditions was done and 1,6-dibromohexane (177.21 mg, 0.726 mmol) and TBAB (20 mg, 0.03 mmol) were added and kept at 80 °C for 1 h. Then Zn (15 mg, 0.227 mmol) was introduced again into the reaction mixture and refluxed for 16 h at 80 °C. Checking the TLC indicated 2 major spots and 2 faint spots in between with no starting material. Extraction was performed using diethyl ether (4 × 10 mL) and water (5 × 10 mL). The organic layer later was quenched with saturated aqueous ammonium chloride solution and the extraction of organic layer was again performed using diethyl ether (4 × 10 mL) twice. The combined organic layers were dried over anhydrous Na<sub>2</sub>SO<sub>4</sub> and then the evaporation of the solvent was

executed under vacuum in a rotary evaporator. The reaction mixture was subsequently purified using column chromatography with ethyl acetate/hexane (1/9 v/v) as eluent and the first major spot and the second major spot was collected with a yield of ~ 15% and ~ 30% respectively.

From the NMR of the first spot, it was observed that the peak corresponding to the methyl group next to Br was missing instead there was a terminal CH<sub>3</sub> peak (with 6 protons) which indicates that the spot corresponds to 4,8-bis(hexyloxy)benzo[1,2-b:4,5-b']dithiophene (**6**) which was obtained as white sticky solid with a yield of 21%. The NMR of the second major spot suggests that the desired compound, 4,8-Bis[(6-bromohexyl)oxy]benzo[1,2-b:4,5-b']dithiophene (**5**) was formed in the reaction and isolated as a white solid with a yield of 38%.

**<sup>1</sup>H-NMR (400 MHz, CDCl<sub>3</sub>) of 4,8-Bis[(6-bromohexyl)oxy]benzo[1,2-b:4,5-b']dithiophene (**5**):**  $\delta$  (ppm) = 7.47-7.46 (d,  $J$  = 4 Hz, 2 H), 7.38-7.37 (d,  $J$  = 4 Hz, 2 H), 4.30-4.27 (t,  $J$  = 8 Hz, 4 H), 3.46-3.43 (t,  $J$  = 8 Hz, 4 H), 1.97-1.86 (m, 8 H), 1.65-1.54 (m, 8 H).

**<sup>1</sup>H-NMR (400 MHz, CDCl<sub>3</sub>) of 4,8-bis(hexyloxy)benzo[1,2-b:4,5-b']dithiophene (**6**):**  $\delta$  (ppm) = 7.48-7.47 (d,  $J$  = 4 Hz, 2 H), 7.37-7.36 (d,  $J$  = 4 Hz, 2 H), 4.29-4.26 (t,  $J$  = 8 Hz, 4 H), 1.89-1.85 (m, 4 H), 1.59-1.57 (m, 4 H), 1.38 (s, 4 H), 1.25 (s, 4 H), 1.25 (s, 4 H), 0.94-0.90 (m, 6 H).

Due to less yield, some optimizations were performed to obtain only the desired product 4,8-Bis[(6-bromohexyl)oxy]benzo[1,2-b:4,5-b']dithiophene (**5**) rather than the undesired de-protected product 4,8-bis(hexyloxy)benzo[1,2-b:4,5-b']dithiophene (**6**).

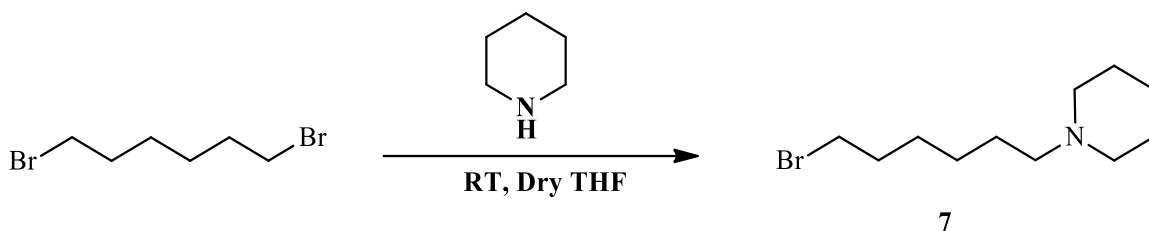
**Table 4.1. Various standardization methods to prepare 4,8-Bis[(6-bromohexyl)oxy]benzo[1,2-b:4,5-b']dithiophene .**

| Reagents  | Conditions  | Observations  |
|---|---|---|
| <ul style="list-style-type: none"> <li>EtOH, H<sub>2</sub>O</li> <li>NaOH (20%)</li> <li>Zn (added in two portions, first 2 equivalents were added and after the addition of 1,6-dibromohexane and TBAB and keeping it for reflux for 1 hour, another 1 equivalent was added).</li> </ul> | <ul style="list-style-type: none"> <li>Reflux for 24 h at 80 °C after the addition of 1,6-dibromohexane.</li> </ul> | <ul style="list-style-type: none"> <li>After the addition of ethanol into the solution the colour gradually gets converted from yellow to deep red.</li> <li>After 16 h of refluxing the colour change was from red to orange-brown.</li> <li>From TLC only 1 major spot and 3 minor spots including starting material were observed.</li> <li>1 major spot correspond to 4,8-bis(hexyloxy)benzo[1,2-b:4,5-b']dithiophene (<b>6</b>) compound.</li> </ul> |



|  |   |  |
|--|---|--|
| <ul style="list-style-type: none"> <li>• DMSO, H<sub>2</sub>O</li> <li>• NaOH (15%)</li> <li>• Zn was added once before the addition of 1,6-dibromohexane and TBAB.</li> </ul> | <ul style="list-style-type: none"> <li>• Reflux for 16 h at 80 °C after the addition of dibromohexane.</li> </ul>     | <ul style="list-style-type: none"> <li>• The colour conversion from yellow to red was observed.</li> <li>• After 1 h the colour turned from red to greenish yellow.</li> <li>• After the addition of 1,6-dibromohexane dissolved in DMSO and TBAB, the colour changed to deep red again.</li> <li>• After the end of the reaction the colour of the reaction had turned into orangepink.</li> <li>• On TLC, 2 major spots and 2-3 minor spots in between were observed with no starting material.</li> <li>• The upper major spot correspond to 4,8-bis(hexyloxy)benzo[1,2-b:4,5-b']dithiophene (<b>6</b>) and the secondmajor spot correspondto 4,8-Bis[(6-bromohexyl)oxy]benzo[1,2-b:4,5-b']dithiophene (<b>5</b>).</li> </ul>                         |
| <ul style="list-style-type: none"> <li>• DMSO, H<sub>2</sub>O</li> <li>• NaOH (10%)</li> <li>• Zn was added once before the addition of 1,6-dibromohexane and TBAB.</li> </ul> | <ul style="list-style-type: none"> <li>• Reflux for 16 h at 80 °C after the addition of 1,6-dibromohexane.</li> </ul> | <ul style="list-style-type: none"> <li>• The colour change from yellow to red was observed after the addition of NaOH.</li> <li>• After 1 h the colour changed from red to greenish yellow.</li> <li>• After the addition of 1,6-dibromohexane dissolved in DMSO and TBAB, the colour turned to deep red again.</li> <li>• After the end of the reaction the colour of the reaction had turned into orangepink.</li> <li>• In TLC, only 1 major spot and 3 minor spots in between were observed with no starting material.</li> <li>• The major spot correspond to 4,8-Bis[(6-bromohexyl)oxy]benzo[1,2-b:4,5-b']dithiophene (<b>5</b>).</li> <li>• No 4,8-bis(hexyloxy)benzo[1,2-b:4,5-b']dithiophene (<b>6</b>) spot was observed this time.</li> </ul> |

#### 4.3.5. Synthesis of 1-(6-bromohexyl)piperidine

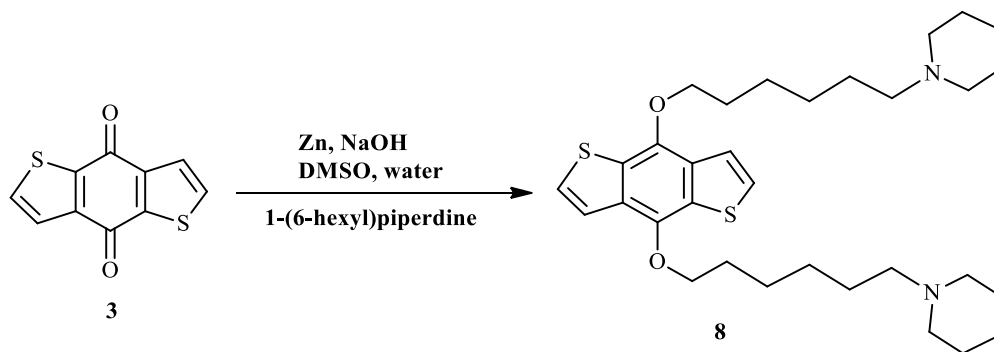


**Scheme 4.5.** Synthesis of 1-(6-bromohexyl)piperidine (7).

In the solution containing 1,6-dibromohexane (1 g, 4.09 mmol) in dry THF (20 mL), slow addition of piperidine (0.38 g, 4.49 mmol) was performed under nitrogen environment. The stirring of reaction mixture was executed for 24 h at RT. After the reaction got completed, the evaporation of the solvent was rendered under reduced pressure by rotary evaporator. The as-resulted residue (white precipitate) was washed with water ( $3 \times 10$  mL) and ethyl acetate ( $2 \times 10$  mL) and the combined organic phases were acidified to pH 1 with hydrochloric acid. The aqueous layer was basified with NaOH solution until the reaction mixture was distinctly basic and then the mixture was subjected again to ethyl acetate extraction ( $3 \times 10$  mL). The drying of combined organic phases was performed over anhydrous  $\text{Na}_2\text{SO}_4$  and its evaporation under reduced pressure. The crude product 1-(6-bromohexyl)piperidine was received as a pale yellow oil with a yield of 95% that was directly used for the next reaction without further purification.

**$^1\text{H-NMR}$  (400 MHz,  $\text{CDCl}_3$ ):**  $\delta$  (ppm) = 3.33-3.30 (t,  $J = 8$  Hz, 4 H), 2.28 (s, 2 H), 2.20-2.17 (t,  $J = 8$  Hz, 2 H), 1.78-1.76 (d,  $J = 8$  Hz, 4 H), 1.50-1.48 (t,  $J = 8$  Hz, 2 H), 1.41-1.33 (m, 6 H), 1.25-1.16 (m, 2 H).

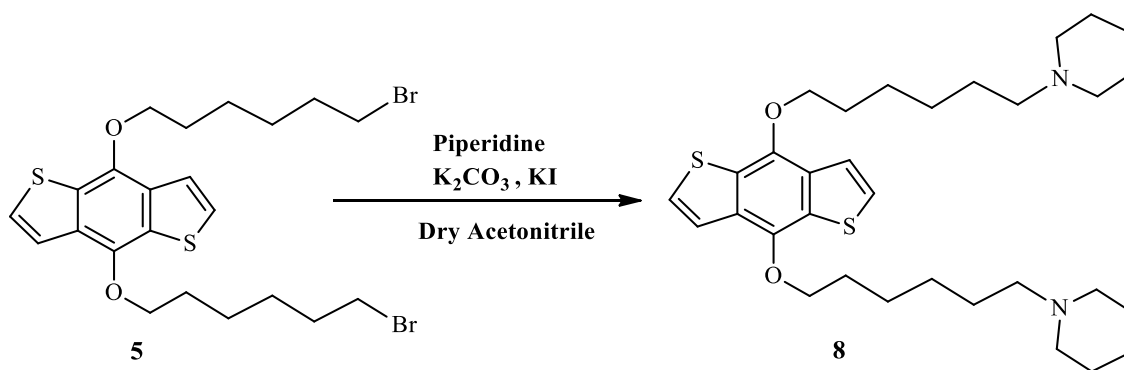
#### 4.3.6. Synthesis of 4,8-Bis(6-(1-hexyloxy)piperidine)benzo[1,2-b:4,5b']dithiophene



**Scheme 4.6.** Synthesis of 4,8-Bis(6-(1-hexyloxy)piperidine)benzo[1,2-b:4,5b']dithiophene (8).

Benzo[1,2-b:4,5-b']dithiophene-4,8-dione (**3**) (50 mg, 0.227 mmol), zinc powder (44.52 mg, 0.681 mmol), 10 mL of water, and 4 mL of DMSO (dimethyl sulfoxide) were put into a 50 mL RB flask; then 600 mg NaOH was introduced into the reaction mixture. The stirring of the mixture was well-executed under nitrogen atmosphere and kept for refluxing for 2h. Subsequently, 1-(6-bromohexyl)piperidine (199.52 mg, 0.635 mmol) and a catalytic amount of TBAB were added into the RB flask. After refluxing for 2 h, the color of the reaction mixture gets converted from deep red to greenish yellow. After reflux for additional 16 h, the reaction mixture, with yellow to orange color, was cooled and drained into cold water (6 × 10 mL) and extraction with 40 mL of diethyl ether was performed. The drying of the combined ether layer was performed over anhydrous Na<sub>2</sub>SO<sub>4</sub> and then evaporation of solvent was rendered under vacuum in a rotary evaporator. TLC was checked after workup and there were many spots above the starting material and a major spot below the starting material. Then the purification of reaction mixture was executed using column chromatography with ethyl acetate/ hexane (1/9 v/v) as eluent and the 2 fractions above BDT and dark spot (pure ethyl acetate was used to get the dark spot below BDT) was separated. From <sup>1</sup>H NMR it was concluded that the compound had several extra peaks and from the <sup>13</sup>C NMR, the carbon peaks next to nitrogen was not present. Hence the desired product was not formed.

#### 4.3.7. Synthesis of 4,8-Bis(6-(1-hexyloxy)piperidine)benzo[1,2-b:4,5b']dithiophene



**Scheme 4.7.** Synthesis of 4,8-Bis(6-(1-hexyloxy)piperidine)benzo[1,2-b:4,5b']dithiophene (**8**).

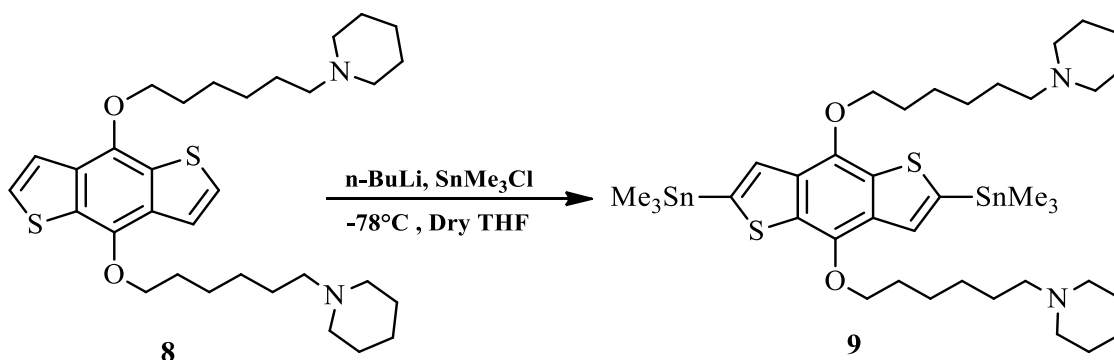
BDT-dibromo-O-alkylated compound (**5**) (30 mg, 0.053 mmol) was mixed with K<sub>2</sub>CO<sub>3</sub> ( 8.78 mg, 0.0636 mmol) and KI (0.1 mg) and then dry acetonitrile (20 mL) was charged into the RB flask containing these reactants. Subsequently, piperidine (10 mg, 0.117 mmol) was introduced slowly to the reaction mixture at 65 °C and then kept for stirring at this temperature overnight.

Subsequently, the evaporation of solvent was executed under reduced pressure and then it was extricated with ethyl acetate (4 × 10 mL) and water (2 × 10 mL) twice. The obtained organic layer was quenched with NaHCO<sub>3</sub> solution and then was dried over anhydrous MgSO<sub>4</sub> and concentrated under reduced pressure to give the crude product. From the TLC, the formation of a polar compound was observed with little amount of un-reacted starting material. The purification of reaction mixture was performed using column chromatography with chloroform/methanol (9/1 v/v) as eluent to obtain the pure product in the form of yellow solid with a yield of 41%.

**<sup>1</sup>H NMR (400 MHz, CDCl<sub>3</sub>):** δ (ppm) = 7.46 (d, *J* = 4 Hz, 2 H), 7.38 (d, *J* = 4 Hz, 2 H), 4.28 (t, *J* = 8 Hz, 4 H), 2.64 (s, 4 H), 2.53 (t, *J* = 8 Hz, 4 H), 1.90-1.83 (m, 4 H), 1.77-1.68 (m, 12 H), 1.63-1.57 (m, 8 H), 1.52 (s, 4 H), 1.45-1.39 (m, 4 H).

**<sup>13</sup>C NMR (100 MHz, MeOD):** 145.60, 132.78, 131.49, 127.64, 121.15, 74.75, 59.61, 54.99, 31.40, 28.16, 27.00, 26.45, 25.63, 24.31.

#### 4.3.8. Synthesis of 1,1'-[4,8-bis[(6-(1-hexyloxy)piperidine)benzo[1,2-*b*:4,5-*b'*]]dithiophene-2,6-diyl]bis[1,1,1-trimethyl-stannate



**Scheme 4.8.** Synthesis of donor molecule with piperidine targeting group.

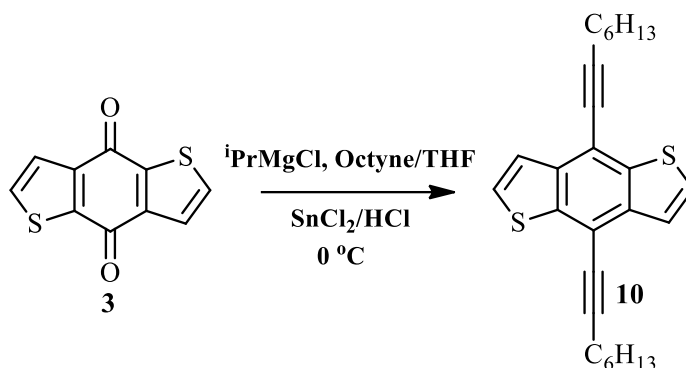
4,8-Bis(6-(1-hexyloxy)piperidine)benzo[1,2-*b*:4,5-*b'*]dithiophene (**8**) 50 mg (0.089 mmol) was taken in a schlenk tube and was mixed in dry THF and then was degassed with 5-6 freeze-pump-thaw degassing cycles. Then the solution was cooled to -78 °C and addition of 0.246 mL (0.493 mmol) of *n*-BuLi (2.0 M solution in hexane) was performed drop wise while stirring under nitrogen environment and the reaction mixture was kept for stirring at -78 °C for 1 h following the addition of 0.5 mL (0.493 mmol) of trimethyltin chloride (1 M solution in hexane). The stirring of reaction mixture was executed overnight at room temperature. The reaction was

quenched by adding water and extraction was performed via ethyl acetate ( $4 \times 10$  mL) and certain quantity of un-reacted starting material was still left in the mixture. Compound **9** was received as white crystalline solid upon recrystallization from ethanol solution with a yield of ~8%. Since compound **8** is highly polar, it was difficult to dissolve the whole amount in THF for the above reaction therefore many other aprotic solvents were used instead of THF in several trial reactions.

**Table 4.2. Various optimization methods for the synthesis of 1,1'-[4,8-bis[(6-(1-hexyloxy)piperidine]benzo[1,2-b:4,5-b']dithiophene-2,6-diyl]bis[1,1,1-trimethyl-stannate.**

| Reagents   | Observation  |
|--|--|
| <ul style="list-style-type: none"> <li>Dry DMF (used as solvent)</li> </ul>          | <ul style="list-style-type: none"> <li>Only starting material was present.</li> </ul>          |
| <ul style="list-style-type: none"> <li>Dry acetonitrile (used as solvent)</li> </ul> | <ul style="list-style-type: none"> <li>1 spot above starting material was observed.</li> </ul> |

#### 4.3.9. Synthesis of 4,8-Di(oct-1-yn-1-yl)benzo[1,2-b:4,5-b']dithiophene



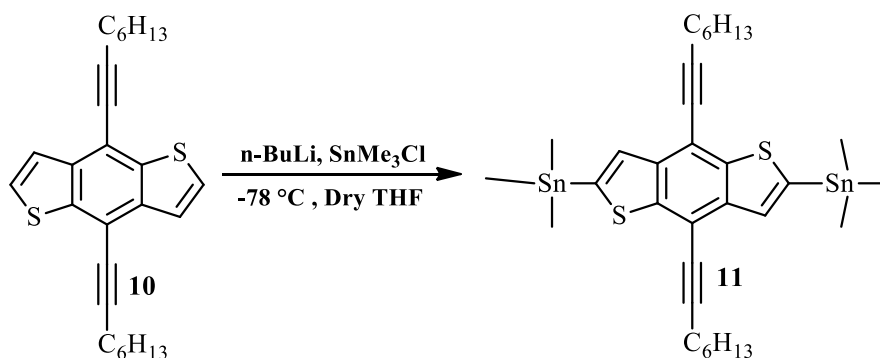
**Scheme 4.9.** Synthesis of alkylated Benzodithiophene.

The addition of isopropylmagnesium chloride (2 M in THF, 1.2 mL, 2.3971 mmol) was performed dropwise to 1-octyne (0.29 g, 2.6315 mmol) at 0 °C. Then the heating of the reaction mixture to 60 °C was executed and kept for stirring for 100 min. It was cooled to RT, and addition of benzo[1,2-b:4,5-b']dithiophene-4,8-dione (**3**) (100 mg, 0.454 mmol) (which was already degassed with 5-6 freeze-pump-thaw cycles) was charged into the reaction mixture. Again it heating was carried out upto 60 °C and kept for stirring for 120 min. It was then cooled to RT, and the addition of 0.7 g of SnCl<sub>2</sub> in HCl solution (16 mL, 10%) was carried out in a dropwise manner to the reaction mixture. The heating of reaction mixture was performed at 65 °C for 60 min and subsequently kept for cooling to room temperature and then charged into

water (4 × 10 mL) where extraction was performed with hexane (6 × 10 mL) twice. The organic fraction was dried over anhydrous Na<sub>2</sub>SO<sub>4</sub> and evaporation was carried out under vacuum using rotary evaporator. Light yellow solid product was recrystallized from the ethanol solution of the crude compound with a yield of 35%.

<sup>1</sup>H NMR (400MHz, CDCl<sub>3</sub>): δ (ppm) = 7.58 (d, *J* = 8 Hz, 2 H), 7.50 (d, *J* = 4 Hz, 2 H), 2.63 (t, *J* = 8 Hz, 4 H), 1.73-1.68 (m, 4 H), 1.38-1.25 (m, 12 H), 0.94-0.86 (m, 6 H).

#### 4.7.10. Synthesis of (4,8-di(oct-1-yn-1-yl)benzo[1,2-b:4,5-b']dithiophene-2,6-diyl)bis(trimethylstannane)

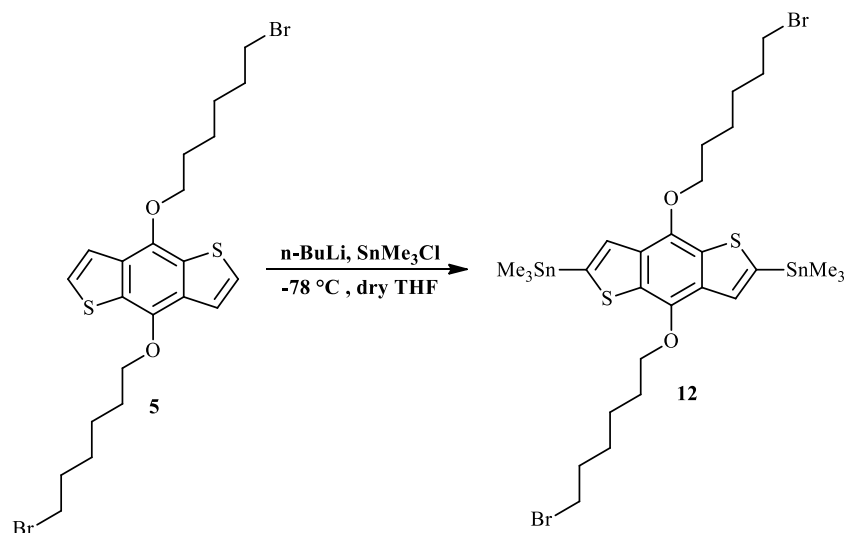


**Scheme 4.10.** Synthesis of (4,8-di(oct-1-yn-1-yl)benzo[1,2-b:4,5-b']dithiophene-2,6-diyl)bis(trimethylstannane) donor molecule with no targeting group.

A solution of compound **10** 100 mg (0.49 mmol) introduced in dry THF was kept for cooling to -78 °C with the dropwise addition of 1.2 mL (1.97 mmol) of n-BuLi (1.6 M solution in hexane) into the reaction mixture while stirring under nitrogen environment. The stirring of reaction mixture was carried out at -78 °C for 1 h which was then followed by introduction of 1.97 mL (1.97 mmol) of trimethyltin chloride (1 M solution in hexane). The reaction mixture was kept for overnight stirring at room temperature. The reaction was quenched by adding water (4 × 10 mL) and extricated with diethyl ether (3 × 10 mL) from which the drying of the obtained combined organic layers was carried out over sodium sulphate with the removal of solvent under reduced pressure using rotary evaporator. Compound **11** was obtained as yellow crystalline solid upon recrystallization from ethanol solution of the crude product with a yield of 60%.

<sup>1</sup>H NMR (400MHz, CDCl<sub>3</sub>): δ (ppm) = 7.61 (s, 2 H), 2.65 (t, *J* = 6.8 Hz, 4 H), 1.72-1.53 (m, 18 H), 0.95-0.92 (m, 6 H), 0.45 (t, *J* = 28 Hz, 18 H).

#### 4.3.11. Synthesis of 1,1'-[4,8-bis[(6-bromohexyl)oxy]benzo[1,2-*b*:4,5-*b'*]dithiophene-2,6-diyl]bis[1,1,1-trimethyl-stannate



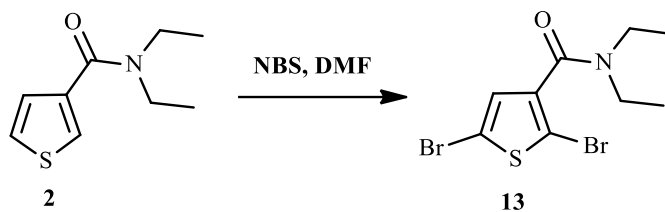
**Scheme 4.11.** Synthesis of 1,1'-[4,8-bis[(6-bromohexyl)oxy]benzo[1,2-*b*:4,5-*b'*]dithiophene-2,6-diyl]bis[1,1,1-trimethyl-stannate (**12**).

Compound **5** (50 mg, 0.091 mmol) was taken in a schlenk tube and dissolved in dry THF which was then degassed with 5-6 freeze-pump-thaw degassing cycles. Subsequently, the cooling of the solution was carried out to  $-78^{\circ}\text{C}$ . Dropwise addition of 0.25 mL (0.5 mmol) of *n*-BuLi (2.0 M solution in hexane) was performed while stirring under nitrogen atmosphere and the reaction mixture was kept for stirring at  $-78^{\circ}\text{C}$  for 1 h followed by addition of 0.5 mL (0.5 mmol) of trimethyltin chloride (1 M solution in hexane). The overnight stirring of reaction mixture was performed at room temperature and subsequently quenched by adding water and extracting it with diethyl ether. TLC of the mixture showed two spots above starting material and also significant quantity of unreacted starting material was retained. Compound **12** was received as yellowish white crystalline solid upon recrystallization from ethanol solution with a 5% yield.

**Table 4.3.** Various optimization methods for the synthesis of 1,1'-[4,8-bis[(6-bromohexyl)oxy]benzo[1,2-*b*:4,5-*b'*]dithiophene-2,6-diyl]bis[1,1,1-trimethyl-stannate.

| Reagents   | Observations  |
|--|---|
| <ul style="list-style-type: none"> <li><math>n\text{-BuLi}</math> (2.2 eq and 4.4 eq)</li> </ul> | <ul style="list-style-type: none"> <li>No reaction</li> <li>Only starting material was left</li> </ul>                                |
| <ul style="list-style-type: none"> <li><math>n\text{-BuLi}</math> (5.5-6 eq)</li> </ul>          | <ul style="list-style-type: none"> <li>2 spots formed above starting material</li> <li>Starting material was also present.</li> </ul> |

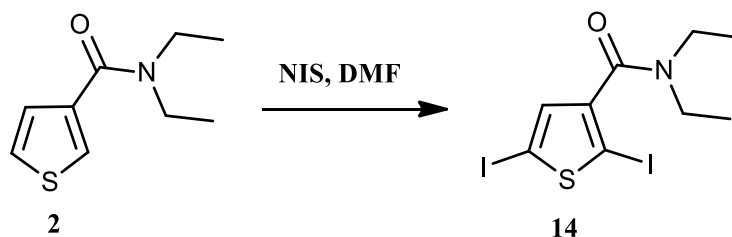
#### 4.7.12. Synthesis of 2,5-Dibromo-N,N-diethylthiophene 3-Carboxamide



**Scheme 4.12.** Synthesis of 2,5-Dibromo-N,N-diethylthiophene 3-Carboxamide.

In the solution of 200 mg (1.09 mmol) of compound **2** in 20 mL of DMF, addition of N-bromosuccinimide (407.83 mg, 2.29 mmol) was executed slowly, followed by stirring at room temperature for 8 h. The solution was charged into 50 mL of cold water and extricated with 60 mL of diethyl ether. The collected organic phase was washed several times with brine to remove the DMF, dried with Na<sub>2</sub>SO<sub>4</sub> and evaporation was carried out under reduced pressure to get the crude product as yellowish oil. TLC was checked after the workup and 3 spots were observed with no starting material. These 3 spots could be the tri-, di- and mono-bromosubstituted compounds and could not be isolated by column chromatography owing to their negligible R<sub>f</sub> difference.

#### 4.3.13. Synthesis of 2,5-Diiodo-N,N-diethylthiophene 3-Carboxamide



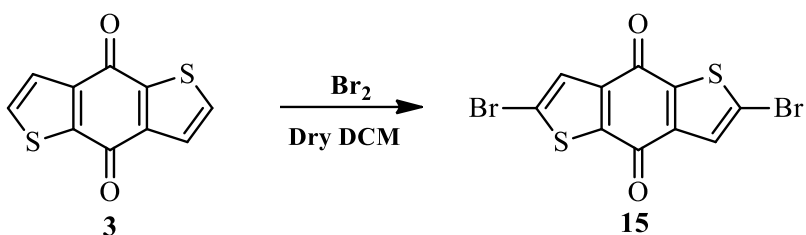
**Scheme 4.13.** Synthesis of 2,5-Diiodo-N,N-diethylthiophene 3-Carboxamide.

In a solution of 105 mg (0.476 mmol) of compound **2** in 20 mL of DMF, the addition of N-iodosuccinimide (214.5 mg, 0.953 mmol) of was carried out slowly, following the stirring at room temperature for 10 h. The solution was drained into 50 mL of cold water and extraction was performed with 60 mL of diethyl ether. The collected organic phases were washed several times with cold water and brine to remove the DMF, dried with Na<sub>2</sub>SO<sub>4</sub> and evaporation was executed under reduced pressure in a rotary evaporator to get the crude product as dark brown



oil. After checking the NMR, only starting material was found to be present in the reaction mixture.

#### 4.3.14. Synthesis of 2,6-Dibromobenzo[1,2-b;4,5-b']dithiophene-4,8-dione



**Scheme 4.14.** Synthesis of 2,6-Dibromobenzo[1,2-b;4,5-b']dithiophene-4,8-dione.

In the solution of Benzo[1,2-b;4,5-b']dithiophene-4,8-dione (**3**) (50 mg, 0.227 mmol) in 20 mL dry DCM, dropwise addition of Br<sub>2</sub> (101.5 mg, 0.59 mmol) was carried out under nitrogen environment at room temperature. Subsequently, the reaction was kept for stirring for 24 h at room temperature. The organic layer was extorted with 40 mL DCM and the excess bromine was quenched by adding saturated Na<sub>2</sub>SO<sub>3</sub> solution and 50 mL water. The extrication was done thrice and the combined organic layers were dried over anhydrous Na<sub>2</sub>SO<sub>4</sub> and evaporation was performed under reduced pressure to give the crude product. After checking the TLC, four spots were formed with 2 major spots including starting material. Since there were many spots observed including starting material, several other reaction conditions were tried in order to standardize the synthesis.

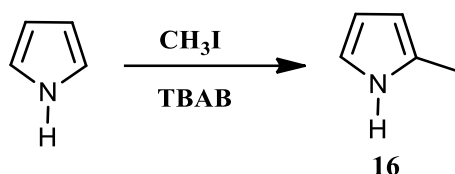
**Table 4.4. Various standardization methods (trial reactions) to prepare 2,6-Dibromobenzo[1,2-b;4,5-b']dithiophene-4,8-dione (15).**

| Brominating Reagents Added   | Conditions   | Observations   |
|--|--|--|
| <ul style="list-style-type: none"> <li>BDT (50 mg, 0.227 mmol)</li> <li>Br<sub>2</sub> (0.231 mL, 0.452 mmol)</li> </ul>                                   | <ul style="list-style-type: none"> <li>Stirred at RT for 24 h</li> </ul> | <ul style="list-style-type: none"> <li>Only starting material was left.</li> </ul>     |
| <ul style="list-style-type: none"> <li>BDT (50 mg, 0.227 mmol)</li> <li>NBS (125 mg, 0.681 mmol)</li> <li>Acetic acid (1 mL, dropwise addition)</li> </ul> | <ul style="list-style-type: none"> <li>Stirred at RT for 24 h</li> </ul> | <ul style="list-style-type: none"> <li>Only starting material was observed.</li> </ul> |
| <ul style="list-style-type: none"> <li>BDT (50 mg, 0.227 mmol)</li> <li>NBS (117 mg, 0.658 mmol)</li> </ul>  | <ul style="list-style-type: none"> <li>Stirred at RT for 24 h</li> </ul> | <ul style="list-style-type: none"> <li>Only starting material was observed.</li> </ul> |

|  |   |  |
|--|---|--|
| <ul style="list-style-type: none"> <li>• BDT (50 mg, 0.227 mmol)</li> <li>• CBr<sub>4</sub> (226 mg, 0.681 mmol)</li> <li>• n-BuLi (0.28 mL, 2M in hexane)</li> <li>• Dry THF</li> </ul> | <ul style="list-style-type: none"> <li>• Dropwise addition of n-BuLi to a solution of BDT dissolved in dry THF at -78 °C for 30-45 min.</li> <li>• Then CBr<sub>4</sub> was added to the solution at RT then kept for stirring for 12 h at RT.</li> </ul> | <ul style="list-style-type: none"> <li>• Multiple spots were observed with some starting material.</li> <li>• Not a clean reaction.</li> </ul> |
|--|---|--|

### 4.3.15. Synthesis of 2-methyl pyrrole

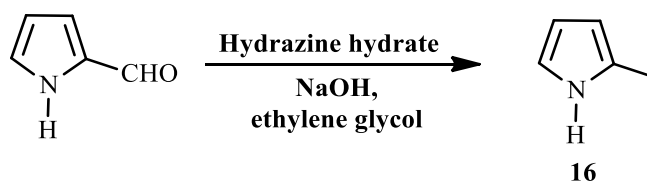
#### Procedure 1



**Scheme 4.15.1.** Synthesis of methyl pyrrole.

Pyrrole (283.11 mg, 4.22 mmol), CH<sub>3</sub>Br (200 mg, 1.404 mmol) and catalytic amount of TBAB were mixed under nitrogen in dark conditions at 40 °C for 3 h. The spots were not able to be identified or isolated by TLC therefore crude NMR was recorded which showed only the starting material peaks, hence the reaction failed.

#### Procedure 2



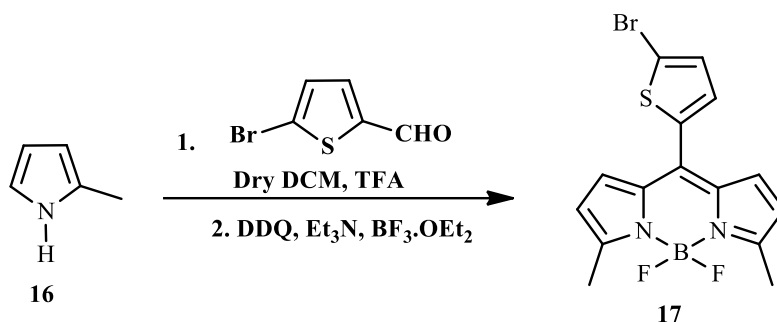
**Scheme 4.15.2.** Synthesis of methyl-pyrrole.

A dissolution of Pyrrole 2-carboxyaldehyde (500 mg, 5.25 mmol) in ethylene glycol (30 mL) and then NaOH (1.09 g, 27.405 mmol) and hydrazine hydrate (1.03 g, 32.445 mmol) was introduced under nitrogen environment which was then kept for stirring at 200 °C for 5 h. During the reaction, the organic phase was distilled using a standard distillation set up in order to receive the pure compound. The reaction mixture was extricated using brine solution (4 × 10 mL) and DCM (3 × 10 mL) twice and then the organic layers were dried over anhydrous Na<sub>2</sub>SO<sub>4</sub> and the solvent

was concentration was performed via rotary evaporator. The TLC showed only one spot with no starting material. Pure compound was retained in the form of yellow oily liquid with a yield of 83%.

$^1\text{H NMR}$  (400MHz,  $\text{CDCl}_3$ ):  $\delta$  (ppm)= 7.96 (s, 1 H), 6.66-6.65 (m, 1 H), 6.13-6.10 (m, 1 H), 5.90 (s, 1 H), 2.28 (s, 3 H).

#### 4.3.16. Synthesis of 8-(2-bromothien-5-yl)-3,5-dimethyl-4,4-difluoro-4-bora-3a,4a-diaza-s-indacene

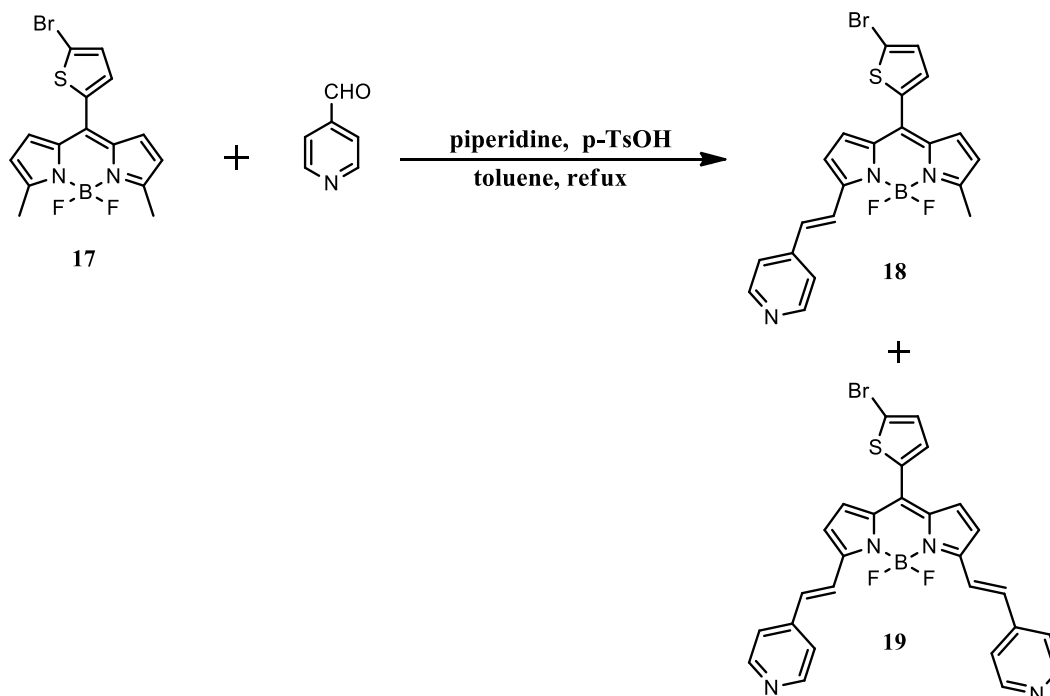


Scheme 4.16. Synthesis of BODIPY Acceptor 17.

In the solution of 5-bromo-2-thiophenecarbaldehyde (400 mg, 2.09 mmol) and 2-methylpyrrole (16) (508.62 mg, 6.27 mmol) in dry  $\text{CH}_2\text{Cl}_2$  (40 mL), addition of trifluoroacetic acid (TFA) (2 drops) was performed slowly under nitrogen environment, and the stirring of the mixture was carried out at ambient temperature overnight. Next, the addition of 2,3-dichloro-5,6-dicyano-1,4-benzoquinone (DDQ) (474 mg, 2.09 mmol) was carried out, and the reaction mixture was kept for stirring for additional 2.5 h. Finally, triethylamine ( $\text{Et}_3\text{N}$ ) (1.69 g, 16.72 mmol) and boron trifluoride diethyl etherate ( $\text{BF}_3\cdot\text{Et}_2\text{O}$ ) (1.77 g, 12.54 mmol) were charged into the reaction system, and then was kept for stirring for 2 h. The reaction mixture was drained into water ( $4 \times 10$  mL) and extorted with  $\text{CH}_2\text{Cl}_2$  ( $8 \times 10$  mL). The combined organic layers were extorted 5 times and was then dried over  $\text{Na}_2\text{SO}_4$ , filtered and concentrated under vacuum using rotary evaporator to give a crude product, whose purification was performed by column chromatography on silica gel using  $\text{CH}_2\text{Cl}_2$ /Hexane (2/1 v/v) as the eluent. The pure product was retained as a crystalline red solid with a yield of 37%.

$^1\text{H NMR}$  (400MHz,  $\text{CDCl}_3$ ):  $\delta$  (ppm)= 7.18 (s, 2 H), 7.05 (d,  $J = 4$  Hz, 1 H), 6.99 (s, 1 H), 6.31 (d,  $J = 4$  Hz, 2 H), 2.64 (s, 6 H).

**4.3.17. Synthesis of 10-(5-bromothiophen-2-yl)-5,5-difluoro-3,7-bis((E)-2-(pyridin-4-yl)vinyl)-5H-dipyrrolo[1,2-c:2',1'-f][1,3,2]diazaborinin-4-ium-5-uide**



**Scheme 4.17.** Synthesis of Di-styryl BODIPY (**19**) and Mono-styryl BODIPY (**18**) via Knoevenagel Condensation

In the solution of compound **17** (0.05 g, 0.13 mmol) and 4-pyridinecarboxaldehyde (0.05 mL, 0.59 mmol) in dry toluene (15mL), p-TsOH (5 mg), the addition of piperidine (1.7 mL, 17.55 mmol) was performed under a N<sub>2</sub> environment. The refluxing of the reaction mixture was carried out for 12 h at 110 °C taking the help of a Dean-Stark instrument used for water removal generated during the condensation. In the beginning, the color of the reaction was reddish pink. After 4 h, the reaction mixture was red-violet in color and then after 16 h, the color of the reaction gradually turned into greenish black in color. The removal of solvent was performed via the rotary evaporator. TLC showed the absence of starting material with the presence of many spots below starting material. The separation of spots was carried out by column chromatography using CHCl<sub>3</sub>/ MeOH (9/1v/v) however NMR could not be recorded.

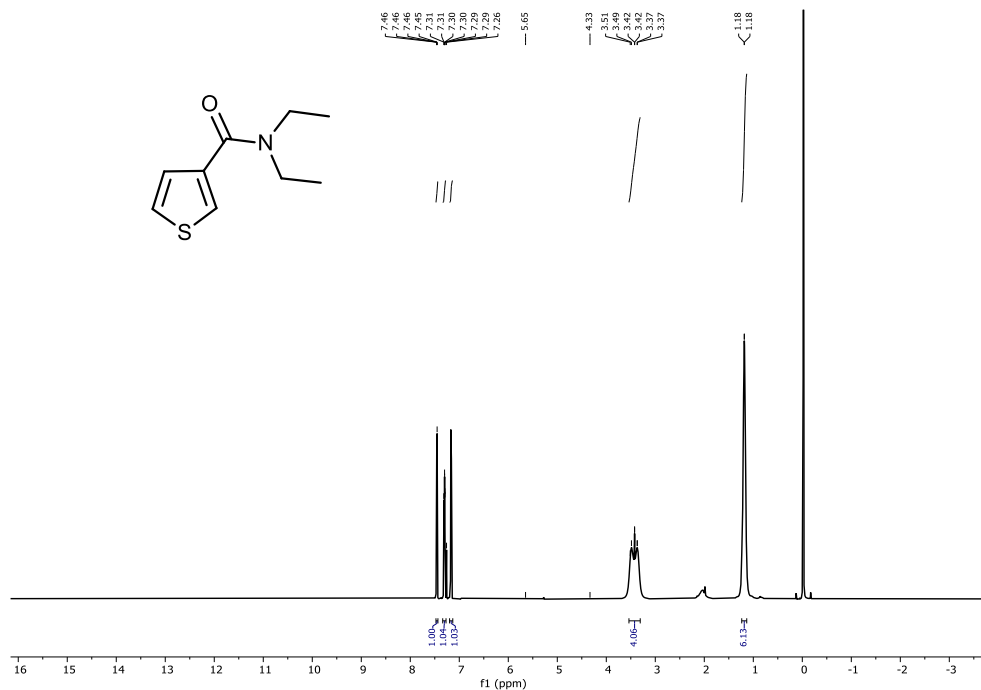
## References

1. Rotkiewicz, K.; Grellmann, K. H.; Grabowski, Z. R., *Chem. Phys. Lett.* **1973**, *19*, 315–318.
2. Sasaki, S.; Drummen, G. P. C.; Konishi, G. I., *J. Mater. Chem. C* **2016**, *4* (14), 2731–2743.
3. Lee, S. C.; Heo, J.; Woo, H. C.; Lee, J.; Seo, Y. H.; Lee, C.; Kim, S.; Kwon O., *Chem. Eur. J.* **2018**, *24*, 13706–13718.
4. Schuddeboom, W.; Jonker, S. A.; Warman, J. M.; Leinhos, U.; Kehnle, W.; Zachariasse, K. A., *J. Phys. Chem.* **1992**, *96*, 10809–10819.
5. Haidekker, M. A.; Theodorakis, E. A., *J. Biol. Eng.* **2010**, *4*(11), 1611-1754. .
6. Vyšniauskas, A.; Kuimova, M. K., *Int. Rev. Phys. Chem.* **2018**, *37*, 2, 259-285.
7. Haidekker, M. A.; Theodorakis, E. A., *Org. Biomol. Chem.* **2007**, *5*, 1669–1678.
8. Grabowski, Z. R.; Rotkiewicz, K.; Rettig, W., *Chem. Rev.* **2003**, *103*, 3899–4032.
9. Sk, B.; Khodia, S.; Patra, A., *Chem. Commun.* **2018**, *54* (14), 1786–1789.
10. Boens, J. N.; Leen, V.; Dehaen, W., *Chem. Soc. Rev.* **2012**, *41*, 1130 – 1172.
11. Kuimova, M. K.; Yahioglu, G.; Levitt, J. A.; Suhling, K., *J. Am. Chem. Soc.* **2008**, *130*, 21, 6672-6673.
12. Haidekker, M. A.; Brady, T. P.; Lichlyter, D.; Theodorakis, E. A., *J. Am. Chem. Soc.* **2006**, *128*, 398–399.
13. Cao, C.; Liu, X.; Qiao, Q.; Zhao, M.; Yin, W.; Mao, D.; Zhang, H.; Xu, Z., *Chem. Commun.* **2014**, *50*, 15811–15814.
14. Amdursky, N.; Erez, Y.; Huppert, D., *Acc. Chem. Res.* **2012**, *45*, 1548–1557.
15. Zhu, H.; Fan, J.; Du, J.; Peng, X., *Acc. Chem. Res.* **2016**, *49*, 2115–2126.
16. Ueno, T.; Nagano, T., *Nat. Methods*, **2011**, *8*, 642–645.
17. Haugland, R. P., *The Molecular Probes Handbook: A Guide to Fluorescent Probes and Labeling Technologies*; Life Technologies: Carlsbad, CA, **2010**.
18. Lesnefsky, E. J.; Moghaddas, S.; Tandler, B.; Kerner, J.; Hoppel, C. L., *J. Mol. Cell Cardiol.* **2001**, *33*, 1065–1089.
19. Napolitano, J. S. M.; Aprille, J. R., *Adv. Drug Delivery Rev.* **2001**, *49*, 63-70
20. Hoye, A. T.; Davoren, J. E.; Wipf, P.; Fink, M. P.; Kagan, V. E., *Acc. Chem. Res.* **2008**, *41*, 87-97.
21. Roopa, Kumar, N.; Bhalla, V.; Kumar, M., *Chem. Commun.* **2015**, *51*, 15614-15628.
22. Chen, L. B., *Annu. Rev. Cell Biol.* **1988**, *4*, 81-155.
23. Dickinson, B. C.; Chang, C. J.; *J. Am. Chem. Soc.* **2008**, *130*, 9638–9639.
24. Poot, M.; Zhang, Y. Z.; Kramer, J. A.; Wells, K. S.; Jones, L.; Hanzel, D. K.; Lugade, A. G.; Singer, V. L.; Haughland, R. P., *J. Histochem. Cytochem.* **1996**, *44*, 1363–1372.
25. Zhang, X.; Sun, Q.; Huang, Z.; Huang, L.; Xiao, Y., *J. Mater. Chem. B*, **2019**, *7*, 2749–2758.
26. Song, X.; Li, N.; Wang, C.; Xiao, Y., *J. Mater. Chem. B*, **2017**, *5*, 360–368.

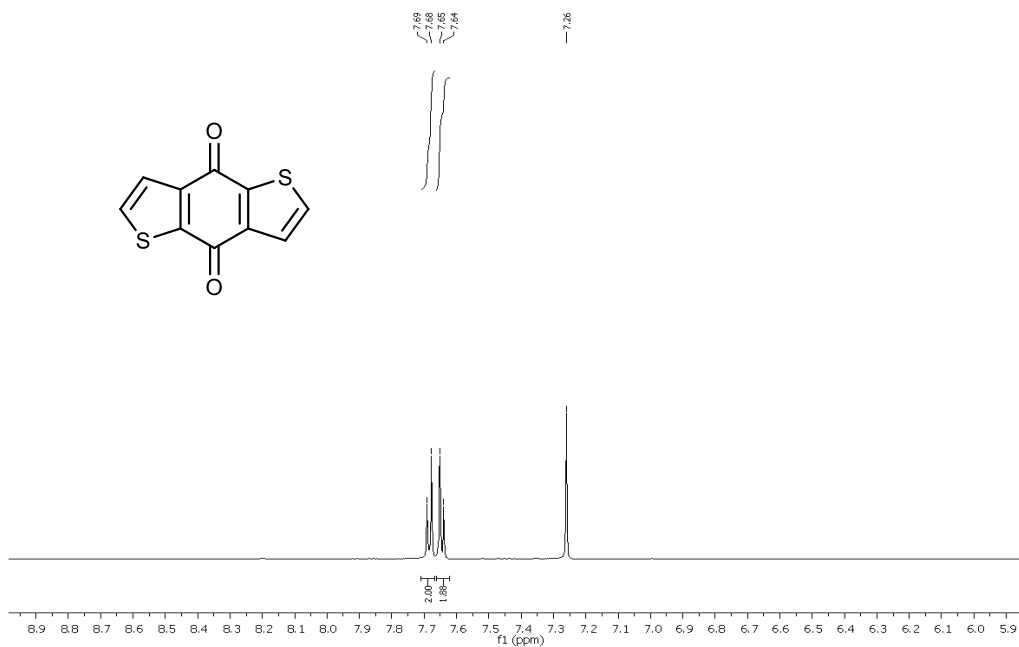
27. (a) Harkness, *J. Biorheology*. **1971**, 8, 93-171. (b) Huizing, M.; HelipWooley, A.; Westbroek, W.; Gunay-Aygun, M.; Gahl, W. A., *Annu. Rev. Genomics Hum. Genet.* **2008**, 9, 359-386.
28. Wang, L.; Xiao, Y.; Tian, W.; Deng, L., *J. Am. Chem. Soc.* **2013**, 135, 2903–2906.
29. de Silva, A. P.; Gunaratne, H. Q. M.; Gunnlaugsson, T.; Huxley, A. J. M.; McCoy, C. P.; Fademacher, J. T.; Rice, T. E., *Chem. Rev.* **1997**, 97, 1515-1566.
30. Yu, H. B.; Xiao, Y.; Jin, L. J., *J. Am. Chem. Soc.* **2012**, 134, 17486.
31. Peng, X.; Wu, T.; Fan, J.; Wang, J.; Zhang, S.; Song, F.; Sun, S., *Angew. Chem.* **2011**, 123, 4266–4269.
32. Ishikawa-Ankerhold, H. C.; Ankerhold, R.; Drummen, G. P. C., *Molecules*, **2012**, 17, 4047–4132.
33. Aswathy, P. R.; Sharma, S.; Tripathi, N. P.; Sengupta, S., *Chem. Eur. J.* **2019**, 25, 14870–14880.
34. Sengupta, S.; Pandey, U. K., *Org. Biomol. Chem.* **2018**, 16 (12), 2033–2038.

# Appendix

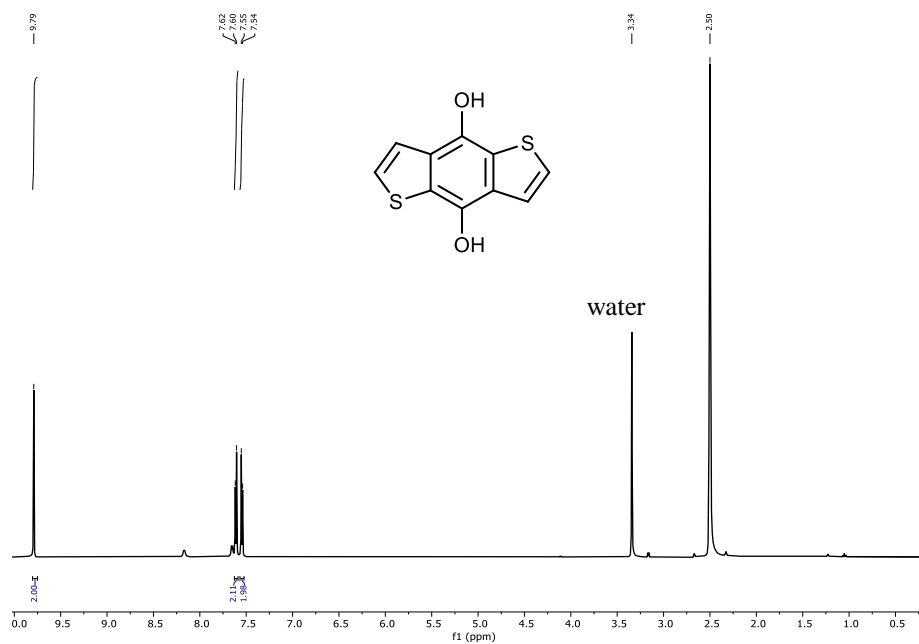
## (*N,N*-diethyl)thiophenecarboxamide, (2), $^1\text{H}$ NMR, $\text{CDCl}_3$ , 400 MHz



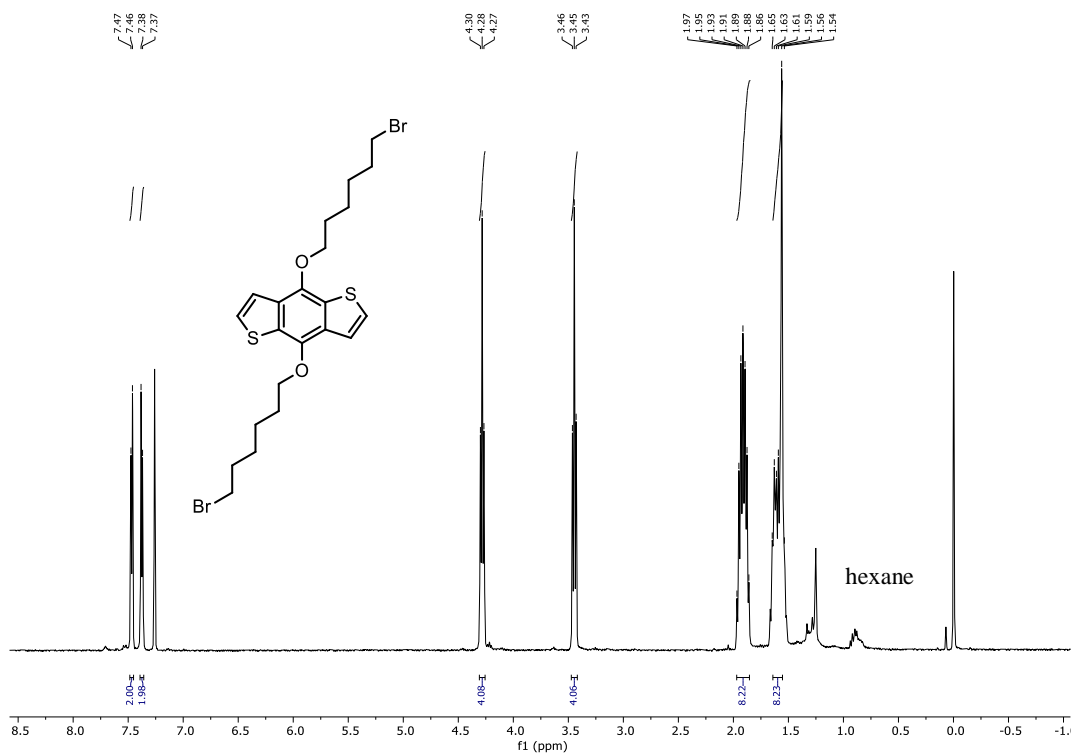
## Benzo[1,2-b:4,5-b']dithiophene-4,8-dione, (3), $^1\text{H}$ NMR, $\text{CDCl}_3$ , 400 MHz



**4,8-Bis(hydroxy)benzo[1,2-b:4,5-b']dithiophene (3),  $^1\text{H}$  NMR, DMSO, 400MHz**

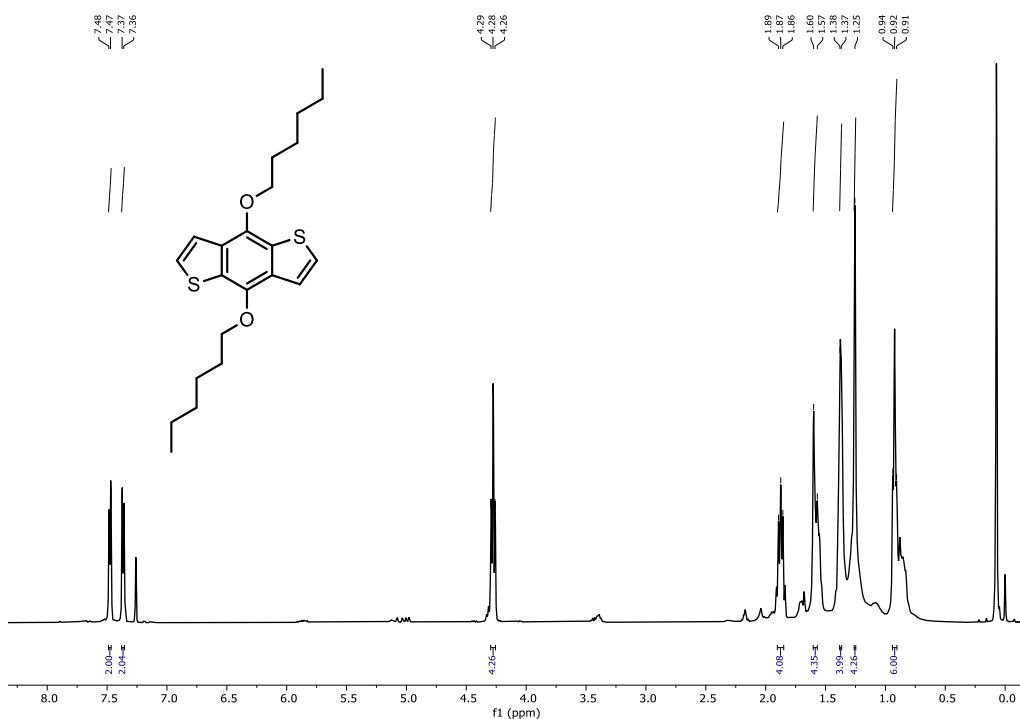


**8-Bis(6-bromohexyl)benzo[1,2-b:4,5-b']dithiophene (5),  $^1\text{H}$  NMR,  $\text{CDCl}_3$ , 400MHz**

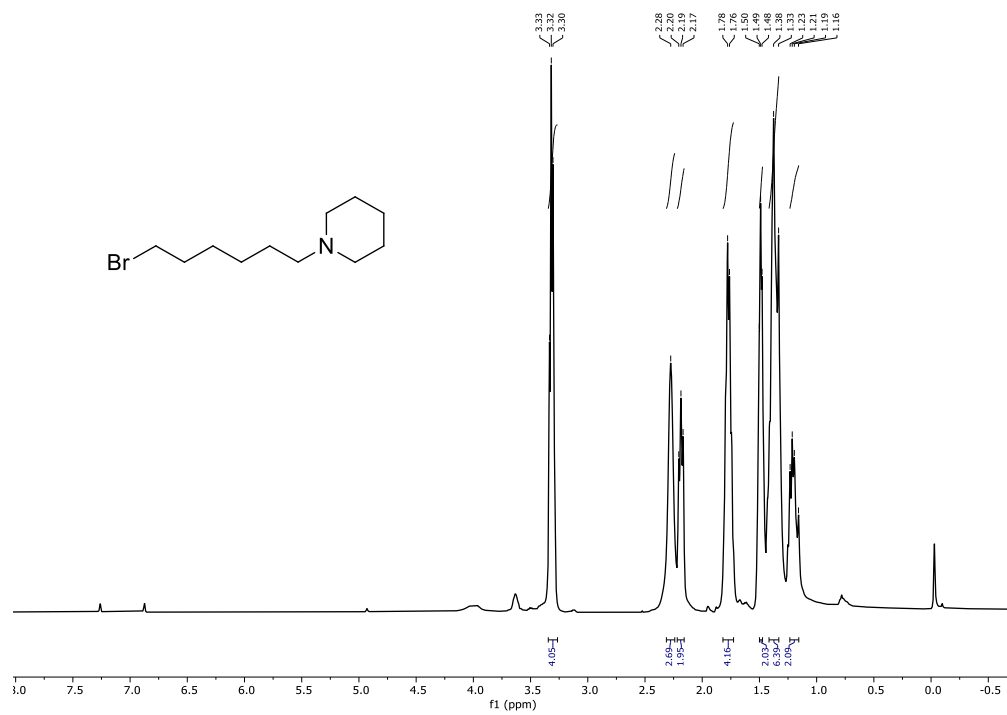




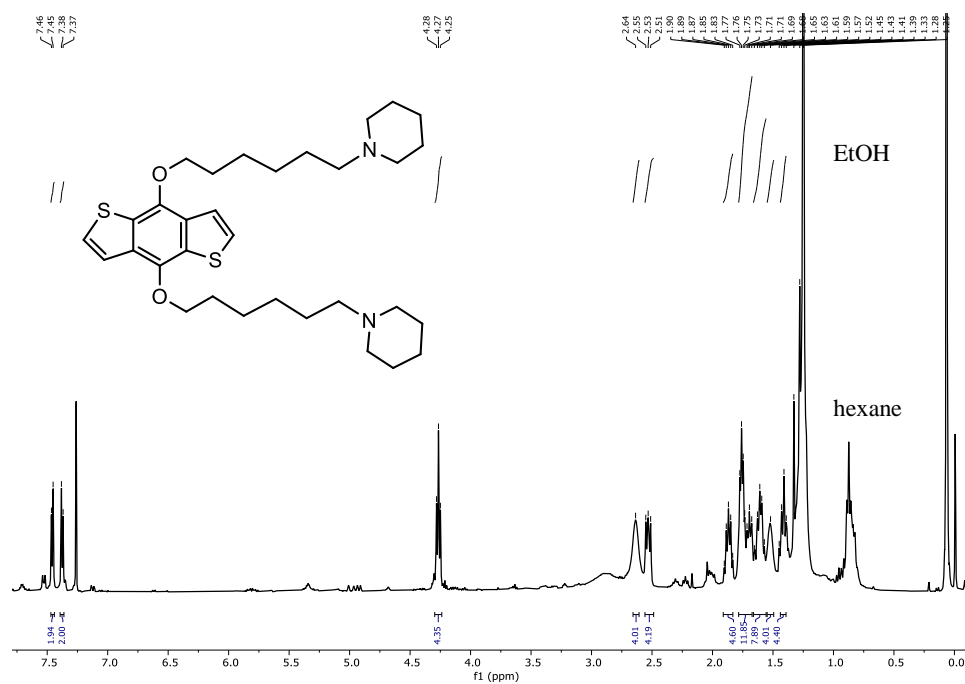
4,8-bis(hexyloxy)benzo[1,2-b:4,5-b']dithiophene (6),  $^1\text{H}$  NMR,  $\text{CDCl}_3$ , 400MHz



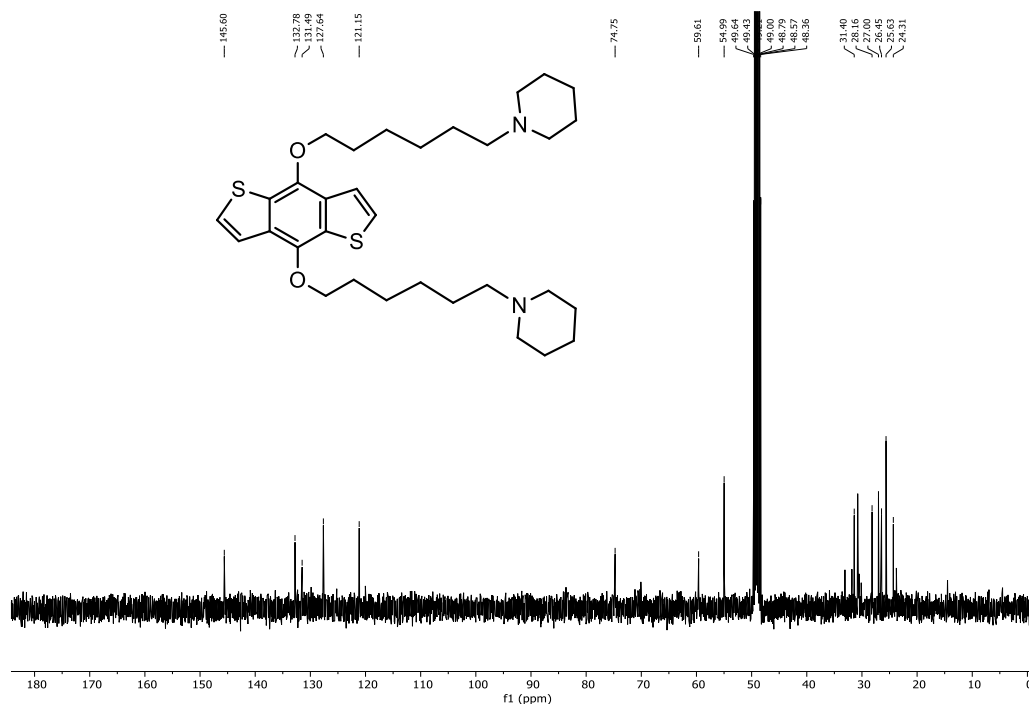
1-(6-bromohexyl)pyridine (7),  $^1\text{H}$  NMR,  $\text{CDCl}_3$ , 400MHz



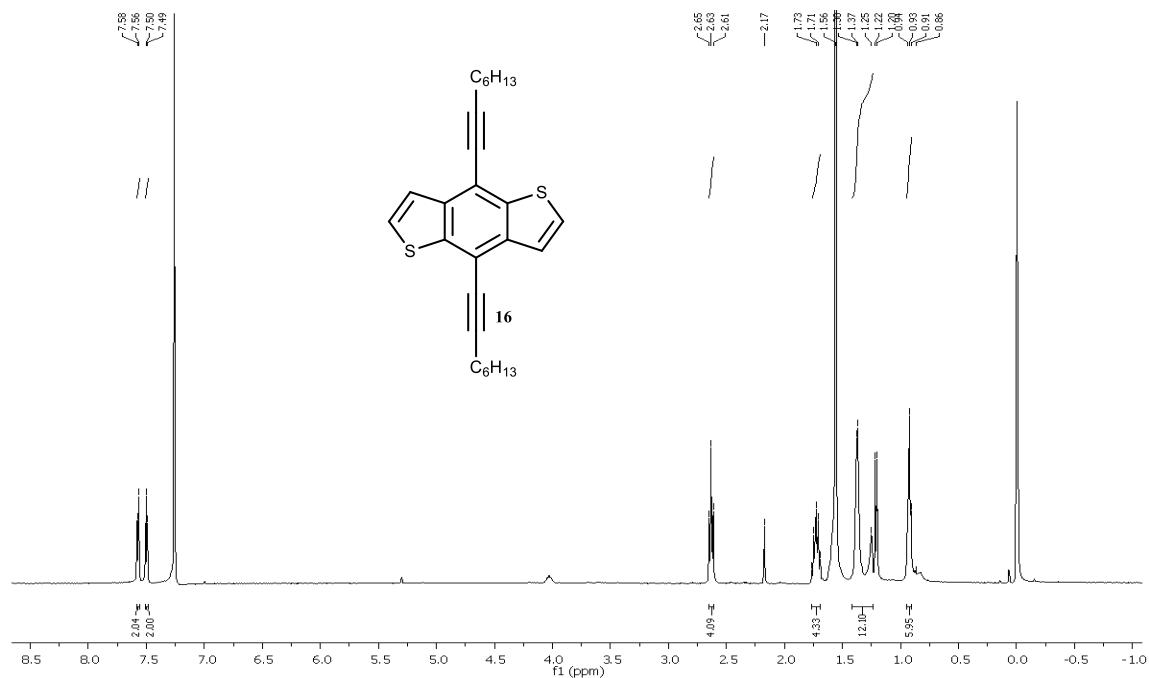
**4,8-Bis(6-(1-hexyloxy)piperidine)benzo[1,2-b:4,5b']dithiophene (8),  $^1\text{H}$  NMR,  $\text{CDCl}_3$ , 400MHz**



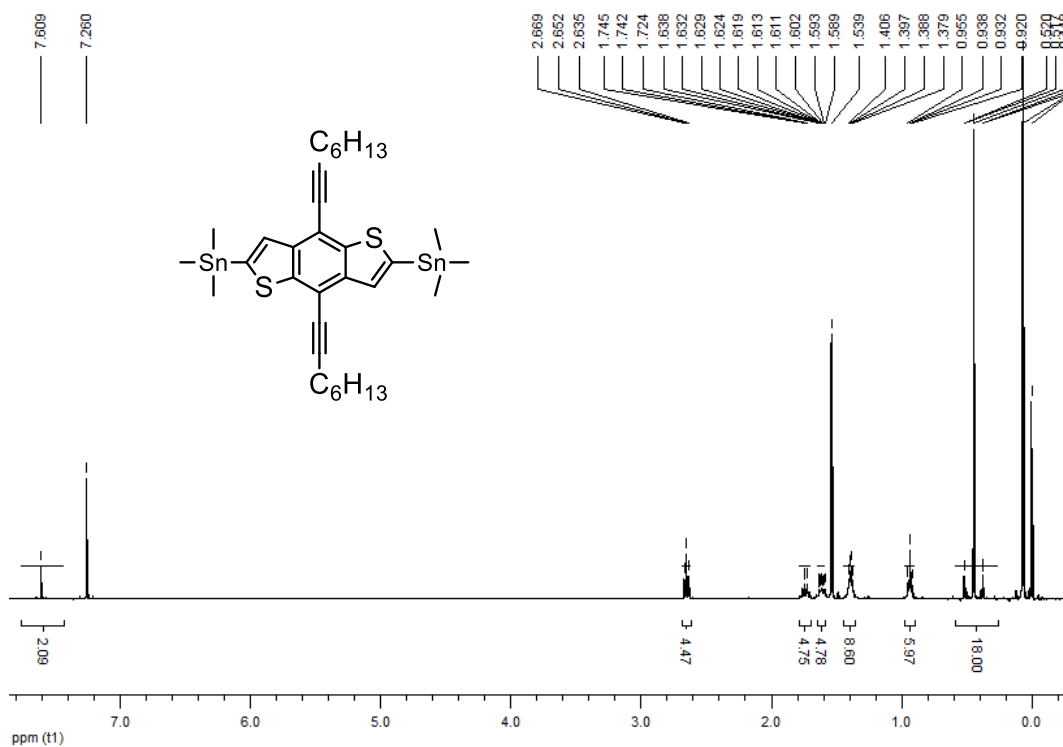
**4,8-Bis(6-(1-hexyloxy)piperidine)benzo[1,2-b:4,5b']dithiophene(8),  $^{13}\text{C}$ -NMR, MeOD, 100MHz**



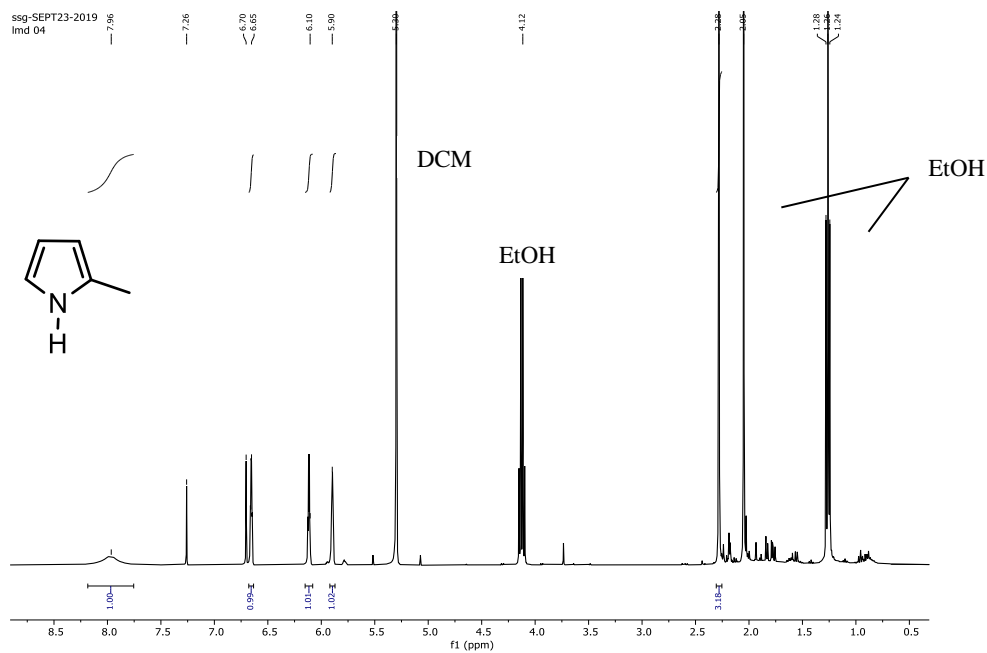
**4,8-Di(oct-1-yn-1-yl)benzo[1,2-b:4,5-b']dithiophene(10),  $^1\text{H}$  NMR,  $\text{CDCl}_3$ , 400MHz**



**4,8-di(oct-1-yn-1-yl)benzo[1,2-b:4,5-b']dithiophene-2,6-diyl bis(trimethylstannane) (11), <sup>1</sup>H NMR, CDCl<sub>3</sub>, 400 MHz**



**2-methyl pyrrole (16), <sup>1</sup>H NMR, CDCl<sub>3</sub>, 400 MHz**



**8-(2-bromothien-5-yl)-3,5-dimethyl-4,4-difluoro-4-bora-3a,4a-diaza-s-indacene (17),  $^1\text{H}$   
NMR,  $\text{CDCl}_3$ , 400 MHz**

